

Accepted Article

***Mycobacterium tuberculosis* RuvX is a Holliday junction resolvase formed by
dimerisation of the monomeric YqgF nuclease domain**

Astha Nautiyal,¹ P. Sandhya Rani,¹ Gary J. Sharples² and K. Muniyappa*¹

¹Department of Biochemistry, Indian Institute of Science, Bangalore 560012, India

²School of Biological and Biomedical Sciences, Biophysical Sciences Institute,
Department of Chemistry, University of Durham, Durham DH1 3LE, United
Kingdom

Running title: *Mycobacterium tuberculosis* Holliday junction resolvase

Key words: Mycobacteria, homologous recombination, DNA repair, Holliday
junction, disulfide-bridge.

*** To whom correspondence should be addressed.**

Tel: +(91-80)-2293-2235/2360-0278

Fax: +(91-80)-2360-0814/0683

E-mail: kmbc@biochem.iisc.ernet.in

This article has been accepted for publication and undergone full peer review but has not been through the copyediting, typesetting, pagination and proofreading process which may lead to differences between this version and the Version of Record. Please cite this article as an 'Accepted Article', doi: 10.1111/mmi.13338

Summary

The *Mycobacterium tuberculosis* genome possesses homologues of the *ruvC* and *yqgF* genes that encode putative Holliday junction (HJ) resolvases. However, their gene expression profiles and enzymatic properties have not been experimentally defined. Here we report that expression of *ruvC* and *yqgF* is induced in response to DNA damage. Protein-DNA interaction assays with purified *M. tuberculosis* RuvC (MtRuvC) and YqgF (MtRuvX) revealed that both associate preferentially with HJ DNA, albeit with differing affinities. Although both MtRuvC and MtRuvX cleaved HJ DNA *in vitro*, the latter displayed robust HJ resolution activity by symmetrically related, paired incisions. MtRuvX showed a higher binding affinity for the HJ structure over other branched recombination and replication intermediates. An MtRuvX^{D28N} mutation, eliminating one of the highly conserved catalytic residues in this class of endonucleases, dramatically reduced its ability to cleave HJ DNA. Furthermore, a unique cysteine (C38) fulfils a crucial role in HJ cleavage, consistent with disulfide-bond mediated dimerization being essential for MtRuvX activity. In contrast, *E. coli* YqgF is monomeric and exhibits no branched DNA binding or cleavage activity. These results fit with a functional modification of YqgF in *M. tuberculosis* so that it can act as a dimeric HJ resolvase analogous to that of RuvC.

Introduction

The central intermediate formed during mitotic and meiotic recombination is a four stranded DNA structure, also known as the Holliday junction (HJ), and its efficient resolution is essential for proper segregation of chromosomes (West, 1997; Kowalczykowski, 2000; Wyatt and West, 2014). HJs are formed between sister chromatids or homologous chromosomes by strand exchange at gaps or breaks in DNA, and also arise by regression of stalled replication forks (McGlynn and Lloyd, 2000; Michel, 2000; Seigneur *et al.*, 1998). In many bacteria, the RuvA, RuvB and RuvC proteins play central roles by virtue of their capacity to promote branch migration and resolution of HJs (Shinagawa and Iwasaki 1996; West 1996). Resolution of HJs is mediated by a diverse group of DNA structure specific endonucleases known as Holliday junction resolvases (HJR) which have been found in a wide variety of organisms based on their shared functional characteristics (Lilley and White, 2001; Wyatt and West, 2014). HJ resolvases are classically homodimeric, metal ion dependent endonucleases that bind preferentially to HJs and catalyze their resolution by symmetrical, paired incisions across the branch point (White *et al.*, 1997; Lilley and White, 2000; Giraud-Panis *et al.*, 1995). A key feature of HJ resolvases is the presence of a cluster of 3-4 negatively charged amino acids, which coordinate the binding of divalent metal ions for phosphodiester bond hydrolysis (Sharples, 2001). HJ resolution by dual strand incision leads to the formation of nicked DNA duplexes that can be restored by DNA ligase (Dunderdale *et al.*, 1991; Iwasaki *et al.*, 1991). *E. coli* RuvC, the founder member of a class of HJ resolvases, exhibits a high degree of structure and sequence selectivity in resolving HJ structures (Shah *et al.*, 1994a).

Bioinformatic analyses of evolutionary relationships among HJ resolvases suggests that HJR function has arisen independently from four distinct structural folds, namely RNase H, endonuclease VII-colicin E and RusA (Aravind *et al.*, 2000). Furthermore, similar analyses of HJRs identified another family within the RNase H fold, along with the previously characterized RuvC family of junction resolvases. This new family of putative HJRs is typified by *E. coli* YqgF protein. The *yqgF* gene is highly conserved among bacterial genomes (Aravind *et al.*, 2000; Ponting, 2002) and, unlike RuvC, is essential for growth of many bacteria, including *E. coli* (Freiberg *et al.*, 2001), *Mycobacterium tuberculosis* (Sasseti *et al.*, 2003) and *Salmonella enterica* serovar *typhimurium* (Hidalgo *et al.*, 2004). Various

studies have found notable structural similarities in the folds of *E. coli* RuvC and YqgF proteins (Fig. S1) despite the latter exists as a monomer in solution (Liu *et al.*, 2003). Utilising homology-based molecular modelling, YqgF is predicted to function as a nuclease in various aspects of nucleic acid metabolism. In *E. coli*, YqgF is involved in antitermination at Rho dependent terminators *in vivo* (Iwamoto *et al.*, 2012) and in 16S rRNA processing (Kurata *et al.*, 2015). However, *Helicobacter pylori* DprB, which belongs to the *E. coli* YqgF family shows HJ binding and resolution activity *in vitro* and promotes recombination and DNA repair *in vivo* (Zhang and Blaser, 2012). These data are consistent with the notion that YqgF may fulfil an important role in the processing of branched DNA recombination intermediates alongside essential functions in RNA metabolism. In the literature and databases, differing nomenclature has been employed to refer to the YqgF/RuvX family of predicted nucleases. For clarity in this study, we use MtRuvX when referring to the *M. tuberculosis* YqgF/RuvX putative HJR.

M. tuberculosis is a major, global human pathogen; however, the molecular mechanism of recombinational DNA repair is not well understood in this organism (McFadden, 1996; Vultos *et al.*, 2009). The annotated genome sequence of *M. tuberculosis* reveals the presence of apparent orthologues of many of the well characterised DNA recombination and repair genes found in *E. coli* (Mizrahi and Andersen, 1998; Muniyappa *et al.*, 2000). As with *E. coli*, HR is important for mediating DNA repair in *M. tuberculosis* (Vultos *et al.*, 2009). However, it is not known whether these putative gene homologues have the ability to encode catalytically active proteins or catalyze biochemical reactions intrinsic to the processes of HR and/or DNA repair. Significantly, it has been suggested that defects in DNA replication, recombination and repair machinery are likely contributors to the evolution of the *M. tuberculosis* genome (Liu *et al.*, 2006; Rosas-Magallanes *et al.*, 2006).

Sequence analysis of the *M. tuberculosis* genome revealed the presence of *ruvC* (Rv2594c) and *yqgF* (Rv2554c) genes that could potentially encode HJ resolvases. Previous studies have demonstrated that *M. tuberculosis ruvC* is induced following DNA damage (Brooks *et al.*, 2001; Rand *et al.*, 2003) and *ruvX* is expressed during the active growth phase of *M. tuberculosis* (Fu and Fu-Liu, 2007). In addition, *Mycobacterium smegmatis ruvC* mutants display an increased sensitivity to moxifloxacin, a fluoroquinolone that inhibits DNA gyrase (Long *et al.*, 2015). In this study, we isolated *M. tuberculosis ruvC* and *yqgF* genes and

purified their respective products, termed MtRuvC and MtRuvX. We found that MtRuvC exhibits HJ binding activity similar to that of MtRuvX, but surprisingly only the latter possessed significant HJ cleavage activity *in vitro*. Further biochemical characterization revealed that MtRuvX exists as a homodimer in solution, exhibits greater binding affinity and specificity for HJ DNA and a higher efficiency of cleavage on a HJ with a homologous core rather than that observed with a fixed, non-homologous HJ substrate. Cleavage sites were mapped on the branch-migratable HJ and were located close to the point of strand crossover and were symmetrically related. Site-directed mutagenesis of Asp28, a catalytic residue highly conserved among RuvC family HJ resolvases (Fig. S1A), dramatically impaired the ability of MtRuvX to catalyze HJ resolution. We also found that disulfide-bond mediated dimerization of MtRuvX plays a crucial role in HJ cleavage. Among all of the known HJRs, this is the first example of a HJR requiring the formation of an intermolecular disulfide-bond for activity. Perhaps this is due to the fact that TB bacilli survive in harsh conditions whereby intermolecular disulfide-bond formation facilitates regulation of the quaternary state of the protein, allowing MtRuvX to fulfil different roles according to the prevailing condition of the cell. Taken together, these findings demonstrate that *M. tuberculosis* YqgF/RuvX is a genuine HJR analogous to RuvC from *E. coli*.

Results

DNA damaging agents induce the expression of M. tuberculosis ruvC and ruvX genes.

One mechanism utilized by organisms to respond to genotoxic agents is to upregulate the transcription of genes for DNA damage tolerance and repair. Previous studies have demonstrated the increase in *M. tuberculosis* *recA* and *ruvC* gene expression in response to treatment with different DNA-damaging agents (Movahedzadeh *et al.*, 1997; Brooks *et al.*, 2001). To assess the involvement of the *M. tuberculosis* *ruvX* gene in the DNA damage response, we examined gene expression levels following exposure to methyl methanesulfonate (MMS) and ultraviolet light. *M. tuberculosis* H37Ra was grown in the absence of any treatment or treated with 0.04% MMS or UV and samples taken at 6, 12, 24, and 48 h. Equal quantities of total RNA collected from the control and cells treated with DNA damaging agents were analyzed for expression of *recA*, *ruvC* and *ruvX* genes by quantitative real-time PCR using the indicated primers (Table S1). Consistent with previous data

(Movahedzadeh *et al.*, 1997; Brooks *et al.*, 2001), the transcriptional levels of *recA* gradually increased in cells exposed to MMS, with an 8.6-fold increase after 48 h (Fig. 1A). Likewise, the transcriptional changes for *ruvC* and *ruvX* were ~6 to 8- fold higher than those for control samples, indicating that these genes are also induced to similar levels following MMS exposure (Fig. 1A). A somewhat consistently lower level of expression was noted for *recA*, *ruvC* and *ruvX* genes in cells exposed to UV radiation but all three are clearly induced by 48 h (Fig. 1B). Together these data show that *ruvX* expression is induced by DNA-damaging agents and that RuvX may therefore participate in recombinational DNA repair in *M. tuberculosis*.

Cloning, expression and purification of M. tuberculosis RuvC and RuvX

To investigate whether the *M. tuberculosis ruvC* gene encodes a functionally active HJR, *ruvC* was amplified by polymerase chain reaction from the cosmid MTCY227, and the product inserted into the expression vector pET43.1a(+) to generate pMtRC (Fig. S2A). A similar expression construct of MtRuvX was amplified by PCR from *M. tuberculosis* genomic DNA and inserted into the pET21a(+) expression vector to create pMtRX (Fig. S2D). Both constructs were verified by restriction digestion and nucleotide sequence analysis.

E. coli strain Rosetta (DE3) pLysS was transformed with pMtRC and pMtRX and expression of each protein induced by addition of IPTG. Analysis of whole cell lysates by SDS-PAGE, followed by Coomassie blue staining, indicated that MtRuvC accumulated in the soluble fraction as a fusion protein of 80 kDa (Fig. S2B), the same was undetectable in the whole cell lysates of cells grown in the absence of IPTG. MtRuvC was purified using a combination of steps, including fractionation on Ni²⁺-NTA agarose, proteolytic removal of the NusA-His₆-tag from the N-terminus of the fusion protein, followed by gel filtration on a Sephadex-75 column (Fig. S2C). The resultant MtRuvC protein was >95% pure as judged by SDS-PAGE (Fig. S2C) and its identity was confirmed by N-terminal sequencing. Analysis of whole cell lysates carrying pMtRX, indicated the presence of MtRuvX in the soluble fraction of cells exposed to IPTG (Fig. S2E). RuvX was purified to homogeneity using sequential chromatographic steps which included SP-Sepharose, heparin-agarose and Sephadex 75 gel filtration columns (Fig. S2F). *M. tuberculosis* RuvX has a predicted molecular mass of 18

kDa which matched that determined by MALDI-TOF mass spectrometry; its identity was also confirmed by N-terminal sequence analysis.

Holliday junction-binding and resolution activities of MtRuvC and MtRuvX proteins

Both RuvC and YqgF proteins are present in a number of bacterial species and multiple sequence alignments suggest a homologous relationship between these two protein families (Aravind *et al.*, 2000). Furthermore, multiple alignment-based secondary structure prediction posits that YqgF family proteins are nucleases with a catalytic mechanism similar to that of archetypal *E. coli* RuvC HJR (Fig. S1; Aravind *et al.*, 2000). Although *Helicobacter pylori* DprB protein, an YqgF homolog, has been shown to bind a synthetic HJ and catalyze its resolution (Zhang and Blaser 2012), a thorough investigation of this potentially important activity has yet to be reported. Moreover, nothing is known about the identity of HJRs and the mechanism underlying HJ resolution in mycobacteria.

We therefore investigated whether MtRuvX possesses HJ-specific DNA binding and resolution activity in direct comparison with MtRuvC. DNA substrates were constructed using the ODNs listed in Table S2 and S3. A synthetic HJ was made by annealing oligonucleotides of 60 nt in length to give a 12 bp homologous core flanked by heterologous arms. HJ recognition by MtRuvC and MtRuvX was assessed in binding mixtures containing a fixed amount of ^{32}P -labeled HJ (0.5 nM) in the presence of increasing concentrations of MtRuvC (200-2000 nM). Binding assays were conducted in the absence of a divalent cation to prevent nuclease activity. Samples were separated in an electrophoretic mobility shift assay (EMSA) and protein-DNA interactions visualized using a phosphorimager. The formation of a complex between HJ and MtRuvC was identified as a single band of reduced mobility (Fig. 2A). The abundance of this complex rose with increasing concentrations of MtRuvC, and no additional protein-DNA complexes were observed even at higher protein concentrations. A similar HJ-binding pattern was also evident when MtRuvX was examined by EMSA at concentrations of 25-400 nM (Fig. 2B). Differences in the migration of protein-DNA complexes between MtRuvC and MtRuvX could be due to differences in the size or shape of these proteins, or the number of subunits bound to the junction. It is significant that considerably higher concentrations of MtRuvC (5-fold excess) were required to reach 50% HJ

binding compared to that of MtRuvX. Hence both MtRuvC and MtRuvX are both HJ binding proteins, with MtRuvX displaying a greater affinity for the four-stranded structure.

We next investigated the ability of MtRuvC and MtRuvX to catalyze HJ resolution in DNA-binding assay buffer in the presence of 10 mM Mg^{2+} . To facilitate direct comparison, we employed the same range of protein concentrations as that used in the HJ binding assays. Reaction mixtures separated by polyacrylamide gel electrophoresis showed that at high protein concentration, MtRuvC generates a small amount of a product migrating at the size of a duplex and consistent with formation of a nicked duplex by HJ resolution (Fig. 2C, lanes 7-9). MtRuvX also generated a nicked duplex product suggesting that it is a genuine HJR. Strikingly, it showed significantly higher cleavage activity than MtRuvC, even at a 36-fold lower protein concentration (Fig. 2D). No other DNA products, such as 1-arm or 3-arm bands were observed during these reactions, indicating that symmetrically-related paired incisions are occurring at the core of the HJ. Together, these experiments demonstrate that binding of MtRuvX and MtRuvC to HJ DNA is independent of the presence of divalent cations and that junction resolution is supported by inclusion of Mg^{2+} ions in the reaction buffer. Similar results were obtained in HJ assays performed with NusA-His₆-tagged MtRuvC (data not shown). In the light of these findings, for further analysis in this study, we focused our efforts on the structural, biochemical and mutational analysis of MtRuvX.

Factors and conditions that influence MtRuvX catalyzed HJ cleavage activity

To further optimize the reaction conditions, we investigated the requirement of divalent cations on the HJ cleavage activity of MtRuvX because (i) divalent cations influence the conformation of HJs and (ii) the HJ specific resolvases studied to date require divalent cations for endonuclease activity. The HJ cleavage activity of MtRuvX was examined in the presence of three different divalent cations under identical experimental conditions. In the absence of a divalent cation, we observed no cleaved DNA product (Fig. 3A, lane 1). On the other hand, a significant amount of duplex was generated in the presence of 2.5 mM Mg^{2+} , which increased at 5 mM and further increase (10 mM) had no measurable effect on the cleavage activity (Fig. 3A, lanes 2-4). Under similar conditions, addition of 2.5 mM Mn^{2+} had an equivalent effect to that of 2.5 mM Mg^{2+} , but further increase inhibited the reaction in a dose dependent manner (Fig. 3A, lanes 5-7). In contrast, MtRuvX showed no cleavage activity in the presence of 2.5-

10 mM Zn^{2+} (Fig. 3A, lanes 8-10). These results are consistent with previous studies showing that HJRs require a divalent cation for HJ cleavage (typically Mg^{2+} or Mn^{2+}), but not for HJ-binding activity (Wyatt and West, 2014). As with *E. coli* RuvC and *Pyrococcus furiosus* Hjr (Shah *et al.*, 1994b; Komori *et al.*, 2000), HJ cleavage activity of MtRuvX was stimulated by alkaline pH, with an optimum between 8 and 8.5 (Fig. 3B, lanes 8-9). MtRuvX showed highest HJ resolution activity at 37 °C and 45 °C (Fig. 3C). Inclusion of NaCl in reactions gradually reduced the MtRuvX cleavage activity from 25-100 mM, with activity completely abolished at 200 mM and above (Fig. 3D).

M. tuberculosis RuvX shows specificity for the Holliday junction over fork and duplex DNA substrates

To explore the DNA structure selectivity of MtRuvX binding, a number of substrates that mimic DNA recombination and replication intermediates were tested alongside a linear duplex control. The six representative substrates used were the HJ (with a 12 bp homologous core) containing four 30 bp arms, a replication fork with three 25 bp arms, a flap structure consisting of two 25 bp duplexes and a 25 nucleotide 3' or 5' flap single strand, a splayed duplex containing a 25 bp duplex with a pair of 25 nt single strands and a 30 bp linear duplex DNA. The substrates were constructed by annealing the synthetic oligonucleotides shown in Table S3, and characterized as described previously (Benson and West, 1994). The composition of the binding mixture was similar to that described above and each substrate (0.5 nM), labeled on a single strand at the 5' end with $[\gamma\text{-}^{32}\text{P}]\text{ATP}$, and was incubated with increasing concentrations of MtRuvX (25-1000 nM). The data showed that nucleoprotein complexes formed between MtRuvX and all of the DNA substrates (Fig. 4), with the abundance of this complex increasing concomitant with the increase in concentration of MtRuvX. However, compared to HJ (Fig. 4A), much higher concentrations of MtRuvX were necessary to shift the majority of each of the other substrates tested (Fig. 4B-F). The limited DNA binding observed at lower MtRuvX concentrations followed by a sudden shift in binding suggests significant positive cooperativity in the assembly of protein subunits.

Quantitative analysis of the extent of complex formation between MtRuvX and these branched DNA structures, as a function of increasing concentrations of MtRuvX, indicated that the half-maximum binding of MtRuvX is achieved at a ~3 to 4-fold lower protein

concentration for the HJ over replication fork and flap-like structures (Fig. 4G). MtRuvX bound weakly to linear duplex DNA, and binding was not saturable (Fig. 4F). The data support an MtRuvX binding preference on these substrates in the order: HJ>replication fork>splayed duplex =flap duplexes >linear duplex DNA. The relative affinities (apparent K_d values) of MtRuvX for the various DNA recombination/replication substrates using EMSA were estimated (Table S4). Assuming a Langmuir 1:1 binding model, the calculated K_d value for HJ is 93.5 nM, which is ~2-fold lower than those of the replication fork and splayed duplexes (Table S4). These findings show that MtRuvX has a clear structure-selectivity of DNA binding with highest affinity for the four-stranded HJ substrate.

To assess further the stability of MtRuvX-DNA complexes we monitored binding to HJ, replication fork and linear duplex, the complexes were challenged with increasing concentrations of NaCl (Fig. 5). The HJ cleavage activity of MtRuvX was although abolished in the presence of 200 mM NaCl (Fig. 3D, lane 7), the HJ-MtRuvX complex was stable in the presence of 250 mM NaCl (Fig. 5A). In contrast, the same amount of salt caused nearly complete dissociation of nucleoprotein complexes formed between MtRuvX and replication fork and linear duplex DNA (Fig. 5B-D). The reduced stability of nucleoprotein complexes formed by MtRuvX with the latter two DNA substrates fits with their lower substrate affinity (Table S4). MtRuvX therefore binds preferentially to the HJ over fork and linear DNA in conditions that more closely resemble the cellular physiological salt concentration.

MtRuvX binds equally well to both immobile and mobile Holliday junctions, but preferentially cleaves the mobile Holliday junction

All of the known HJRs recognize the HJ structure with varying degrees of selectivity (Lilley and White, 2001). Many of the phage HJRs, such as T4 endonuclease VII and T7 endonuclease I, bind and a cleave HJs and many other branched DNA structures (Sharples, 2001). Others, including RuvC, RusA, CCE1 and SpCCE1, are considerably more HJ specific and require particular nucleotide sequences at the junction crossover point for cleavage (Shah *et al.*, 1994a; Chan *et al.*, 1997; White and Lilley, 1996; Oram *et al.*, 1998). Consequently, these HJRs depend on branch migration of HJs so that the required target sequences can be localized at the junction point. For example, *E. coli* RuvC resolves HJs by symmetrically cleaving two of its DNA strands preferentially at the 5'-A/TTT↓G /C-3' cognate sequence

(Shah *et al.*, 1994a). To investigate any nucleotide sequence specificity intrinsic to the MtRuvX resolution activity, we first examined the ability of MtRuvX to bind immobile and mobile HJs using the band shift assay. The mobile HJ contains four arms of 30 bp in length flanking a 12 bp homologous core; whereas, the immobile HJ, which also contains four arms of 30 bp, has a frozen core that cannot branch migrate. We observed that MtRuvX displayed a similar binding pattern and affinity for both mobile and immobile junctions (Fig. 6A and 6B), indicating that the HJ structure alone, irrespective of its ability to branch migrate, is sufficient for stable binding of MtRuvX *in vitro*.

We also investigated the ability of MtRuvX to cleave mobile and immobile HJs as well as linear duplex DNA. In all cases, reaction mixtures contained 0.5 nM ^{32}P -labeled DNA, 10 mM Mg^{2+} and increasing concentrations of MtRuvX (25-500 nM). When mobile HJ was mixed with MtRuvX, we observed the generation of a cleaved product corresponding to that expected for nicked linear duplex DNA, and its intensity increased significantly with the addition of increasing amounts of MtRuvX (Fig. 6C, lanes 2-12). In contrast, no equivalent product was detected over the same range of MtRuvX concentrations using the immobile HJ (Fig. 6D, lanes 2-12). Instead, two other products were noted that are likely to result from asymmetrical junction cleavage, probably by independent single incision events (Fig. 4D), producing a 3-arm structure and a duplex that is likely to contain a single-strand flap. Similar products of asymmetrical resolution are generated by the phage λ Rap branched DNA endonuclease (Sharples *et al.*, 1998). These results show that the mobile HJ is cleaved much more efficiently than the immobile HJ (Fig. 6F) despite both junctions being bound equally well (Fig. 6A and 6B). In addition, they demonstrate that homology is essential for proper resolution and that MtRuvX is likely to require particular sequences within the junction core to carry out paired incisions in opposing strands across the branch point. As expected for an HJ-specific endonuclease, MtRuvX failed to cleave linear duplex DNA, even at the highest concentration tested (Fig. 6E and 6F).

Sequence-specificity of Holliday junction resolution by MtRuvX

The limited resolution activity of MtRuvX on the immobile junction suggests that it may have some specificity in the sequences it cleaves. To identify the precise position of cleavage sites on the mobile HJ, four identical mobile HJs were constructed, each labelled with ^{32}P in a

different strand. These four substrates were individually incubated in the absence or presence of increasing concentrations of MtRuvX. The resulting cleavage products were analyzed using high resolution denaturing PAGE using markers (Maxam and Gilbert, 1980) to locate the position of HJ incision. The results revealed that MtRuvX introduces only one nick on each strand of the mobile HJ and that these cut sites are symmetrically-related across the branch point within the homologous core of the junction (Fig.7). In strands 2 and 4, major cleavage sites were mapped to the sequence 5'-GT↓CC-3' (Fig. 7B and 7D). Minor cleavage sites in strands 1 and 3 corresponded to cleavage at 5'-TT↓GC-3' (Fig. 7A and 7C). These results reveal that MtRuvX is a genuine HJR, cleaving the junction by paired symmetry-related incisions within the 12 bp homologous core (Fig. 7, schematic at the center). In addition, MtRuvX appears to show some degree of sequence selectivity, cleaving both major and minor sites on the 3' side of thymidine residues. The cut sites and extent of cleavage corresponds exactly to those produced by *E. coli* RuvC on a junction with an identical 12 bp mobile core (Bennett *et al.*, 1993).

MtRuvX failed to cleave Holliday junctions lacking thymidine in the homologous core

To ascertain the requirement for thymidine residues for cleavage by MtRuvX, we conducted cleavage assays using a T-less HJ (Fig.S3). For this purpose, we replaced the AT base pairs within the mobile HJ (Fig. S3A) with GC sequences to construct an alternate structure referred to as a T-less HJ (Fig. S3B; Bennett *et al.*, 1993). Assays were carried out alongside the 12 bp mobile HJ12 as a positive control. MtRuvX efficiently cleaved HJ12 (Fig. S3C, lane 1) as observed before, whereas, no cleavage of the T-less HJ was evident under the same reaction conditions (Fig. S3C, lanes 3-13). These results indicate that MtRuvX depends on thymidine residues for cleavage in a similar fashion to that observed with *E. coli* RuvC (Bennett *et al.*, 1993).

A mutation affecting the proposed active site of MtRuvX significantly reduces HJ resolution activity

The well-characterized crystal structure of the *apo* form of *E. coli* RuvC (Ariyoshi *et al.*, 1994) and *Thermus thermophilus* RuvC in complex with HJ DNA (Gorecka *et al.*, 2013), identify the active species as a homodimer with each catalytic center comprised of four highly

conserved carboxylates (D7, E66, D138 and D141 in *E. coli* RuvC), which coordinate binding of Mg^{2+} for phosphodiester bond hydrolysis (Saito *et al.*, 1995). Multiple sequence alignment of MtRuvX from various bacterial species revealed a different arrangement of conserved acidic residues in the YqgF family, although the position of the first and third aspartates is preserved (Fig. S1; Aravind *et al.*, 2000). To further validate the HJ-specific endonuclease activity of MtRuvX, we generated a site directed mutant of one of these conserved aspartic acids, replacing it with asparagines at position 28, to give MtRuvX^{D28N} (Fig. S1A). This mutant is equivalent to the *E. coli* RuvC^{D7N} substitution which abolishes HJ resolution *in vitro* (Saito *et al.*, 1995). Likewise, a D9A mutation in *E. coli* YqgF was defective in cleaving pre-16S ribosomal RNA (Fig. S1A) (Kurata *et al.*, 2015). The mutant RuvX protein was purified (Fig. 8A) following a similar protocol to that employed with the wild-type (Fig. S2F). In an EMSA, MtRuvX^{D28N} formed a single complex with the ³²P-labeled HJ12 substrate, which increased in intensity with the addition of increasing concentrations of MtRuvX^{D28N} (Fig. 8C). Furthermore, the HJ binding affinity displayed by purified MtRuvX^{D28N} was comparable to that of the wild-type protein (Fig. 8B-D). No additional protein-HJ complexes were observed at higher protein concentrations with either wild-type or mutant protein, indicating that the modification introduced into MtRuvX^{D28N} has no significant effect on HJ recognition.

To further investigate the functional significance of the mutation, we investigated whether MtRuvX^{D28N} exhibits any defect in HJ resolution. Similar to the wild-type enzyme (Fig. 8E), MtRuvX^{D28N} cleaved the HJ substrate to generate a product migrating at the same position as the linear duplex in a concentration dependent manner (Fig. 8F). However, MtRuvX^{D28N} produced substantially less product at all concentrations, suggesting that substitution of the conserved aspartic acid with asparagine has a significant adverse effect on HJ resolvase activity (Fig. 8F and 8G). These data support the notion that the HJ cutting activity is intrinsic to MtRuvX, not contributed by any other protein contaminant, and that the conserved aspartate at position 28 is important for HJ resolvase activity.

MtRuvX exists both in vivo and in vitro as a homodimer

The prevailing view is that classic HJR function as homodimers, which ensures the positioning of two active sites for simultaneous, or near-simultaneous, metal-ion induced strand cleavage (Ariyoshi *et al.*, 1994; Sharples, 2001; Gorecka *et al.*, 2013). However,

whether YqgF family proteins are functionally active as dimers or higher order multimers is not known. During MtRuvX purification from *E. coli* whole cell lysates, we observed two species of MtRuvX of ~20 kDa and ~50 kDa eluting from a gel filtration column, and significantly, the ratio between these two species was sensitive to the presence or absence of reducing agent in the buffer. Since the predicted molecular mass of MtRuvX is 18 kDa, we reasoned that MtRuvX might exist in solution as a homodimer. To further investigate this observation, MtRuvX was exposed to mild cross-linking using glutaraldehyde (Habeeb and Hiramoto, 1968) and the protein analyzed by SDS-PAGE. The SDS/PAGE revealed the presence of a 40 kDa dimeric species, even at the lowest concentration of the cross-linking agent, and also small amounts of a larger oligomer (Fig. 9A). Glutaraldehyde also induced the appearance of a faster migrating band below the ~20 kDa MtRuvX (Fig. 9A) that is likely to be an internally cross-linked monomer (Pérez-Martín and de Lorenzo, 1996). To analyze further the dimeric status of MtRuvX without the requirement for cross-linking, MtRuvX was visualized by tapping mode atomic force microscopy (AFM; Bayburt and Sligar, 2002). A representative AFM image of MtRuvX is shown that illustrates small and large forms of the protein (Fig. 9B). Volumes of the visualized proteins were calculated from the AFM images (Edstrom *et al.*, 1990; Yang *et al.*, 2003) and found to match those expected for monomers and dimers of MtRuvX. AFM measurements also revealed that MtRuvX exists predominantly (>70%) as homodimers (n=40).

The oligomeric status of MtRuvX was also investigated under native conditions (Fig. 9C). Whole cell lysates from *M. tuberculosis* H37Ra were prepared under non-reducing conditions and analyzed on a neutral gel. MtRuvX was detected by Western blotting using polyclonal anti-MtRuvX antibodies. Purified MtRuvX was used as an internal control to help identify monomer and dimer species (Fig. 9C, lane 5). A band corresponding to the dimeric species of MtRuvX was observed in the *M. tuberculosis* whole cell lysates (Fig. 9C, lanes 1-4). The absence of a detectable band in the monomer position in these lysates supports the view that MtRuvX exists predominantly in the form of a homodimer under native conditions. Further, MtRuvX analyzed by gel filtration chromatography eluted in two overlapping chromatographic peaks: a major peak with an apparent molecular weight of ~55 kDa and a satellite peak corresponding to a molecular weight of ~25 kDa (Fig. 9D). Although these results indicate that MtRuvX exists predominantly as a homodimer in solution, the anomalous

molecular weight by gel-filtration may be due to the elongated shape of the molecule. The lesser abundance of homodimers under *in vitro* conditions, as opposed to *in vivo*, may be due to insufficient oxidizing conditions.

Disulfide-bond mediated dimerization of MtRuvX is essential for Holliday junction resolution

Analysis of whole cell lysates indicated that the formation of intermolecular disulfide bonds stabilizes the dimeric species of MtRuvX. To experimentally validate this hypothesis, we incubated MtRuvX under oxidized and reduced conditions in the presence of cupric 1,10-phenanthroline and DTT, respectively. Cupric orthophenanthroline (CuP) is a redox catalyst, which has been widely used to study contact interfaces involving cysteine residues (Careaga and Falke, 1992), while DTT serves to reduce disulfide bonds in proteins and peptides. Hence, if dimerization is mediated by intermolecular disulfide bonds, CuP treatment should enhance the formation of disulfide-linked dimers, whereas incubation with DTT should convert the dimers into monomeric species. Exposure of MtRuvX to CuP prior to separation on SDS-PAGE significantly elevated the amount of dimer formed (Fig. 10A, lane 4). Conversely, incubation with DTT resulted in the conversion of all of the dimers into monomers (Fig. 10A, lane 5), while phenanthroline alone had no significant effect on the ratio of monomer and dimer, compared to the untreated control (Fig. 10A, lanes 2 and 3). These results support the view that disulfide bond formation is important in stabilizing intersubunit contacts within the MtRuvX dimer.

Examination of the MtRuvX amino acid sequence revealed the presence of a single cysteine residue at position 38 (Fig. S1A). We generated a cysteine-free variant of MtRuvX, designated MtRuvX^{C38A}, in which the cysteine residue was substituted with alanine to probe the impact of disulfide bonds on the formation of dimers and also on HJ binding and resolution. The mutant protein was expressed in *E. coli* and purified to homogeneity. Under non-reducing conditions, purified MtRuvX^{C38A} migrated as a single band corresponding to a protein monomer (Fig. 10B, lane 2). Unlike the wild-type (Fig. 10A, lane 2), no trace of a dimer band was observed. Moreover, incubation of MtRuvX^{C38A} in either oxidized or reduced conditions with cupric orthophenanthroline or DTT, respectively, had no effect on the monomeric size of the mutant protein (Fig. 10B, lanes 3-4). Together these results provide compelling evidence that the cysteine at position 38 contributes to dimerization of MtRuvX

through the formation of intermolecular disulfide bonds. We next investigated the effect of MtRuvX cysteine mutant on recognition and cleavage of the mobile HJ. MtRuvX^{C38A} was able to bind the HJ (Fig. 8C) in a manner similar to the wild-type MtRuvX (see Fig. 2A), suggesting that the loss of cysteine and/or disulfide bonding has no significant impact on HJ binding activity. However, when we assessed the catalytic activity of cysteine-38 substitution mutation, it showed no HJ resolution activity (Fig. 10D), indicating that disulfide-bond mediated dimerization plays an essential role in MtRuvX catalyzed HJ resolution. Further, HJ resolution by MtRuvX was inhibited by DTT in a dose-dependent manner with a maximal inhibition of >50% at 10 mM (Fig 10 E)

E. coli YqgF is monomeric and shows no cleavage activity on HJ or other recombination or replication intermediates

Genetic and biochemical evidence implicates the *E. coli* YqgF (EcYqgF) gene product in mRNA and rRNA metabolism (Iwamoto *et al.*, 2012; Kurata *et al.*, 2015). To establish whether EcYqgF might fulfil a dual role in RNA and DNA processing, we purified the wild-type protein to homogeneity (Fig. S4A) to assess its activity on branched DNA junctions. The quaternary structure of EcYqgF was analyzed by gel filtration chromatography and a single peak was observed at 15 kDa, corresponding to the predicted molecular mass of 15.2 kDa for an EcYqgF monomer (Fig. S4B); it should be noted that EcYqgF lacks any cysteines in its protein sequence. Previous studies also concluded that EcYqgF exists as a monomer in solution (Liu *et al.*, 2003).

The DNA binding properties of EcYqgF were investigated using 12 bp mobile and immobile HJs, alongside a 3-stranded junction, Y junction, replication fork, 3' flap and splayed duplex substrates (Fig. S5A, S5C and S5E). EcYqgF failed to bind any of these branched DNA substrates, even with 2 μ M protein on HJ12 (Fig. S5A, lane 4). The experiments were repeated with the inclusion of Mg²⁺ or Mn²⁺ ions to evaluate branched DNA cleavage activity (Fig. S5B, S5D and S5F). No nuclease activity was detected with the HJ, flap or replication fork structures suggesting that YqgF is not involved in resolving recombination intermediates in *E. coli* and that this feature is a specific adaptation of certain other members of the YqgF family in organisms such as *M. tuberculosis* (this work) and *H. pylori* (Zhang and Blaser, 2012).

Discussion

Our studies originated from an *in silico* search for genes that encode functional equivalents of the *E. coli* RuvC HJ resolvase in *M. tuberculosis* (Aravind *et al.*, 2000). This analysis revealed that the *M. tuberculosis* genome possesses, in addition to the canonical *ruvC*, a homolog of *yggF* (annotated as *ruvX* in several databases, including Pfam PF03652; Galperin *et al.*, 2015), which is proposed to encode an alternative HJR related to RuvC (Aravind *et al.*, 2000). Analysis of qPCR data suggested that the pattern of *ruvX* gene expression was similar to that of the *ruvC* and *recA* recombination genes, whereby all three genes are induced following DNA damage in *M. tuberculosis* H37Ra. These results suggest a link between the *ruvX* product and a DNA repair process, such as homologous recombination. To enable a systematic functional analysis, we cloned, expressed and purified the gene products of the *M. tuberculosis ruvC* (MtRuvC) and *ruvX* (MtRuvX) genes. Protein-DNA interaction assays with the purified proteins revealed that both proteins bind to HJ DNA, although MtRuvX showed a much higher binding affinity than MtRuvC. In addition, MtRuvC showed only a weak HJ cleavage activity compared to the robust activity observed with MtRuvX. It is possible that MtRuvC requires the presence of the RuvA•RuvB branch migration complex or some other factor to stimulate its activity. The endonuclease activity of MtRuvX was dependent on Mg²⁺ and Mn²⁺ consistent with the known properties of other RNase H family endonucleases and HJ resolvases (Sharples, 2001; Lilley and White, 2001; Nowotny 2009). However, MtRuvX showed much higher activity with Mg²⁺ than Mn²⁺, which is the opposite of that observed with *E. coli* RuvC (EcRuvC) protein (Shah *et al.*, 1994b). Additional experiments showed that MtRuvX exhibits >2-fold higher binding affinity for HJ over other recombination and replication intermediates. EcRuvC actually shows a much higher HJ binding selectivity than this (Benson and West, 1994), although other resolving enzymes, such as RusA and phage RuvC, bind a wide range of substrates, including forks and duplex DNA (Sharples *et al.*, 1994). As with EcRuvC (Dunderdale *et al.*, 1991; Benson and West, 1994), MtRuvX failed to cleave a HJ lacking a branch migratable core or linear duplex DNA. Mapping of the endonuclease cut sites of MtRuvX revealed that HJ cleavage is due to symmetrically related incisions across the branch point, which is a feature shared by classic, homodimeric HJRs (Sharples, 2001; Lilley and White, 2001). Mutation of

a highly conserved aspartate (MtRuvX^{D28N}) present in all YqgF and RuvC families (Figure S1) resulted in a substantially decreased MtRuvX HJ resolution activity, consistent with the idea that both endonucleases share a related catalytic core and cleavage mechanism. Moreover, we found that the single cysteine present in MtRuvX was required for disulfide-bond mediated intermolecular dimerization and HJ resolution activity, suggesting that *M. tuberculosis* RuvX has adapted its YqgF protein to function like a typical RuvC family HJR.

Bioinformatic (Aravind *et al.*, 2000) and structural (Liu *et al.*, 2003) studies suggest that YqgF and RuvC proteins share a similar catalytic core consisting of a cluster of acidic residues that belong to the integrase/RNase H class of endonucleases (Figure S1). It has been proposed that YqgF supplies an alternative HJR (Aravind *et al.*, 2000), however, recent *in vivo* and *in vitro* work with *E. coli* YqgF (EcYqgF) suggests that it is involved in 16S rRNA processing (Kurata *et al.*, 2015) and transcriptional antitermination (Iwamoto *et al.*, 2012), which fits with it being an essential gene in many bacterial species. We examined the activity of purified EcYqgF as part of this study to determine whether it could function in a dual capacity in HJ resolution and RNA metabolism. The experiments performed with a number of HJ and replication fork structures found no evidence that EcYqgF can recognize or resolve any of these branched DNA structures. The protein was also found to be monomeric, unlike the dimeric RuvC, which lends further support to the notion that YqgF in *E. coli* is involved exclusively in RNA processing.

In contrast, another YqgF homologue from *H. pylori*, known as DprB, has been shown to be involved in homeologous transformation and DNA repair *in vivo*. DprB also binds preferentially to HJs and promotes their resolution in a similar fashion to RuvC *in vitro*, cutting strands at precisely the same location as *E. coli* and *H. pylori* RuvC proteins (Zhang and Blaser, 2012). Despite work on DprB providing the first indication that YqgF family proteins could be involved in resolving recombination intermediates, a number of questions were left unanswered with respect to DNA substrate selectivity and the importance of homodimer formation. In this study, we found that MtRuvX like DprB but unlike EcYqgF, share similar activities on DNA. We observed that the structural features of the DNA substrate dictated the binding affinity and stability of nucleoprotein complexes formed by MtRuvX. Although MtRuvX associated with branched and unbranched substrates, complexes with replication fork and linear substrates were considerably less tolerant than the HJ structure

to increasing salt concentrations. Thus MtRuvX may actually possess a high degree of HJ selectivity in the context of intracellular physiological conditions. In fact, many of the activities of MtRuvX are remarkably similar to EcRuvC, including the location of major and minor symmetry related incisions in the HJ with a 12 bp core of homology and the inability to cleave an immobile HJ or one lacking thymidines in the homologous core (Bennett *et al.*, 1993, Benson and West, 1994). However, the MtRuvX DNA binding properties and preference for Mg²⁺ over Mn²⁺ differs significantly from EcRuvC. To confirm that the HJ specific cleavage activity was intrinsic to MtRuvX, we mutated one of the highly conserved acidic amino acids known to be necessary for EcRuvC and EcYqgF endonuclease activity (Saito *et al.*, 1995; Kurata *et al.*, 2015). The mutant protein, MtRuvX^{D28N}, retains HJ binding activity similar to the wild-type, but showed substantially reduced HJ endonuclease activity. Together these results establish that MtRuvX behaves as a genuine HJR resembling the dimeric RuvC protein. Whether MtRuvX can fulfil a dual role in both RNA and DNA processing has yet to be clarified.

Typical HJRs are dimers so that two catalytic centers can be positioned for dual strand scission close to the junction branch point. The crystal structure of *E. coli* RuvC (Ariyoshi *et al.*, 1994) and *Thermus thermophilus* RuvC alone (Chen *et al.*, 2013) or in complex with a synthetic HJ (Gorecka *et al.*, 2013) reveals a homodimeric complex. The *T. thermophilus* HJR is very similar to *E. coli* RuvC (Chen *et al.*, 2013), sharing a well defined dimer interface, stabilized by a number of hydrophobic contacts and polar interactions. The HJ endonuclease activities observed with MtRuvX fits with its ability to form a dimer and, size-exclusion chromatography, AFM imaging and cross-linking experiments confirmed this to be the case. The stability of this dimeric species was sensitive to the presence of reducing agents and this prompted us to investigate the importance of a unique cysteine in MtRuvX that could contribute to homodimer formation. A mutant lacking this cysteine, MtRuvX^{C38A}, bound HJs normally but was entirely defective in HJ resolution (once again confirming that MtRuvX and not contaminating endonucleases was responsible for this activity). Unlike the wild-type MtRuvX, this mutant was incapable of homodimer formation demonstrating that disulfide bond mediates dimerization. Thus, the redox state in the cell may dictate whether MtRuvX is able to function in HJ resolution, fulfilling a potentially important regulatory role in recombinational DNA repair. The fact that MtRuvX exists predominantly as homodimers in

the *in vivo* context provides credence for the existence of such a possibility. These findings introduce a new and exciting element in our quest to understand the identity of the components and mechanism of HJ resolution in *M. tuberculosis*. In addition, they suggest that *M. tuberculosis* has two alternative molecules, RuvC and RuvX, that could resolve Holliday junctions and both are induced in response to DNA damage. Why distinct activities are available and in what scenarios they might be deployed is unclear, although the *H. pylori* DprB does seem to preferentially target recombination intermediates generated during natural transformation (Zhang and Blaser, 2012). Another intriguing possibility is that these endonucleases may target HJ intermediates via alternative branch migration systems.

The identity of the principal branch migration proteins involved in HR in eukaryotes remains elusive (Lilley and White, 2001; Wyatt and West, 2014). In comparison to eukaryotes, the formation of HJs as well as the molecular mechanism underlying branch migration and resolution in bacteria has been extensively characterized (Shinagawa and Iwasaki, 1996; West 1996; 1997). The movement of a HJ along DNA and its resolution proceeds through several stages. The basic components of the process in *E. coli* include RuvA and RuvB, which bind the HJ and promote ATP-dependent branch migration via helical rotation of opposing DNA duplexes (Han *et al.*, 2006). The next step is catalyzed by RuvC which binds the HJ and promotes its resolution by endonucleolytic cleavage (Dunderdale *et al.*, 1991; Iwasaki *et al.*, 1991). The involvement of an alternative HJR activity is not unprecedented. Numerous studies have uncovered different and complementary pathways for HJ migration and resolution in many bacteria, archaea, and eukaryotes. One of these involves RecG, which processes recombination intermediates independently of RuvA, RuvB and RuvC (Lloyd and Sharples, 1993; Whitby *et al.*, 1993). Indeed, the branch migration and resolution activities of RecG and RusA, respectively, have been proposed to function as ancestral HJ processing components in *Aquifex aeolicus* (Sharples *et al.*, 2002). The RuvX and DprB (Zhang and Blaser, 2012) proteins constitute a new sub-class of alternative HJRs with a catalytic mechanism similar to that of RuvC and related nucleases (Aravind *et al.*, 2000). Despite this structural relationship, little is known about their physiological substrates and mode of action, as well as their interaction with the RuvAB and RecG branch migration components. EcYqgF was tested on a HJ containing an 11 bp homologous core in the

presence of EcRecG, ATP and Mg^{2+} but no activation of endonuclease activity was observed (data not shown).

The HJRs present many fascinating evolutionary questions that are only beginning to be addressed. Whereas the members of the RecA recombinase family are highly conserved throughout evolution, the HJRs are diverse. There are intriguing similarities and dissimilarities between the members of HJR subfamilies which may have been acquired during evolution. The precise mechanism of how RuvX (and RuvC) might coordinate with RuvA•RuvB or RecG proteins to promote HJ resolution and restoration of collapsed DNA replication forks in *M. tuberculosis* remains to be investigated. Nevertheless, we report here the first detailed biochemical characterization of MtRuvX and present important insights into the mechanism of HJ resolution, which could be directly linked to the regulation of different DNA metabolic processes, including HR and DNA repair. Overall, this study opens a new avenue in the understanding of HR in this human respiratory pathogen, together with elucidation of the function of some of the uncharacterized genes which may represent a novel set of recombination enzymes.

Experimental procedures

Biochemicals, plasmid DNA, oligonucleotides, bacterial strains and enzymes

Fine chemicals were purchased from GE Biosciences and Sigma; all chemicals used were of analytical grade. Restriction endonucleases, T4 DNA ligase, T4 polynucleotide kinase and Pfu/Pfx polymerases were obtained from Thermo Scientific. [γ - ^{32}P]ATP was purchased from the Bhabha Atomic Research Center, Mumbai or Perkin Elmer. Fast performance liquid chromatography columns were purchased from GE Biosciences. Oligonucleotides (ODN) were purchased from Sigma-Genosys, Singapore or MWG Biotech. *E. coli* strains DH5 α , BL21-CodonPlus and Rosetta (DE3)pLysS, plasmids pET43.1.a(+), pET21a(+) and pT7-7 were purchased from Novagen. The cosmid MTCY227, carrying the *M. tuberculosis* *ruv* region, was obtained from Institut Pasteur, France.

Western blot analysis

M. tuberculosis H37Ra was grown at 37 °C in Middlebrook 7H9 medium (Difco, Sparks, MD, USA) supplemented with 0.2% glycerol, 10% albumin-dextrose-catalase and

0.05% Tween 80 in a shaker incubator at a speed of 180 rpm. Whole cell lysates were prepared as described previously (Thakur *et al.*, 2013). Western blot analysis of whole cell lysates from untreated *M. tuberculosis* H37Ra cells was conducted using polyclonal antibodies raised against MtRuvX as described previously (Sambrook *et al.*, 1989).

UV light and MMS treatment

M. tuberculosis H37Ra was grown at 37 °C in Middlebrook 7H9 medium (Difco, Sparks, MD, USA) supplemented with 0.2% glycerol, 10% albumin-dextrose-catalase and 0.05% Tween 80 in a shaking incubator at a speed of 180 rpm. At an $A_{600\text{nm}}$ of 0.5, MMS was added to a final concentration of 0.04% and incubation continued at 37 °C. In parallel, cells were exposed to a UV fluorescent lamp (UVITEC, Cambridge, UK) at 180 J/m² for 6 min. After exposure, cultures were incubated while being shaken gently at 37 °C in the dark. At various time intervals cells were harvested, washed with 10% Tween 80 and resuspended in lysis buffer (20 mM Tris-HCl, pH 7.5, 100 mM NaCl, 10% glycerol, 2 mM phenylmethane sulfonyl fluoride).

Quantitative real-time PCR

qRT-PCR reactions were performed on untreated *M. tuberculosis* H37Ra cells and those exposed to UV irradiation or MMS. *M. tuberculosis* H37Ra was grown as described above with harvested cells washed with 10% Tween 80 and resuspended in fresh 7H9 medium. Cell pellets were resuspended in 5 ml of protoplast buffer (15 mM Tris-HCl, pH 8, 0.45 M sucrose, 8 mM EDTA) with 4 mg ml⁻¹ lysozyme and incubated for 45 min at 37 °C. The protoplast suspension was subjected to centrifugation for 10 min at 3000 g. Total RNA was isolated using an RNeasy-kit (Qiagen). This was followed by synthesis of cDNA using a Maxima First Strand cDNA Synthesis Kit (Thermo Scientific) with 1 µg of RNA template as specified by the manufacturer (Thermocycler conditions: 25 °C for 10 min; 65 °C for 15 min and termination of the reaction at 85 °C for 5 min). Real-time PCR assays were conducted with 200 ng of cDNA template, 10 µl of 2X SYBR Green mastermix (Thermo Scientific), 1 µl of forward and reverse primers (5 µM of each) in a StepOnePlus Real-Time PCR machine (Applied Biosystems). Table S1 details the oligonucleotides used for qRT-PCR. The program used for PCR consisted of 10 min of initial denaturation at 95 °C, followed by 40 cycles of 95

°C for 15 sec, primer annealing at 60 °C for 30 sec, extension at 72 °C for 30 sec followed by the melting curve.

DNA substrates

The sequence of oligonucleotides used for the preparation of DNA substrates used in this study are listed in Table S2 and S3. Oligonucleotides were labeled at the 5' end by [γ -³²P] ATP and T4 polynucleotide kinase (Sambrook *et al.*, 1989). DNA substrates were prepared by annealing different combinations of oligonucleotides (ODNs), as shown in Table S3. For each substrate, stoichiometric amounts of purified ODNs were annealed in 100 μ l of 0.3 M sodium citrate, pH 7, 3 M NaCl. ODN mixtures were heated for 5 min at 95 °C followed by slow cooling to 4 °C over a period of 2 h. Annealed substrates were electrophoresed on a 12% (w/v) polyacrylamide gel in 89 mM Tris-borate buffer (pH 8.3) containing 1 mM EDTA. Bands were excised from the gel and eluted into TE buffer (10 mM Tris-HCl, pH 7.5, 1 mM EDTA).

Construction of a recombinant plasmid carrying the M. tuberculosis ruvC gene

The nucleotide sequence of the *ruvC* gene (accession number, Rv2594c) was identified using the TubercuList database (<http://www.Pasteur.fr/Bio/TubercuList>). The coding sequence corresponding to *M. tuberculosis* H37Rv *ruvC* gene (Rv2594c) was amplified via PCR from the cosmid MTCY 227 using 5'-ATGGGATCCGTGCGGGTGATGGGTGTC-3' and 5'-ATGCTCGAGTCATCGGGCGGCCTTCAG-3' carrying BamHI and XhoI restriction sites (underlined), respectively. The PCR product was gel purified, digested with BamHI and XhoI and inserted into the pET-43.1a(+) expression vector to give pMtRC.

Purification of M. tuberculosis RuvC

MtRuvC protein was expressed in the *E. coli* strain Rosetta (DE3)pLysS harbouring pMtRC. Bacteria were grown in LB broth supplemented with antibiotics (100 μ g ml⁻¹ ampicillin and 34 μ g ml⁻¹ chloramphenicol) at 37 °C until the A_{600nm} reached 0.5. MtRuvC was induced by addition of 0.5 mM IPTG and cultures further incubated while being shaken gently at 18 °C for 12 h. Cells were harvested by centrifugation, washed in STE buffer (10 mM Tris-HCl, pH 8, 100 mM NaCl, 1 mM EDTA), resuspended in buffer A (20 mM Tris-HCl, pH 8, 50 mM NaCl, 10% glycerol, 5 mM 2-mercaptoethanol) and stored at -80 °C. Cells were thawed,

sonicated (model No. GEX-750, ultrasonic processor) and the suspension was centrifuged in a Beckman Ti-45 rotor at 104350 x g for 1 h at 4 °C. The whole cell lysate was applied onto a Ni²⁺-NTA agarose column pre-equilibrated with buffer A. Bound proteins were eluted with a 50-500 mM linear gradient of imidazole in buffer A. Fractions containing MtRuvC were pooled and dialyzed against buffer B (20 mM Tris-HCl, pH 7.5, 10 % glycerol) containing 50 mM NaCl. Enterokinase (Sigma) was added to the dialyzate and cleavage carried out at 4 °C for 12 h. Removal of the affinity tag from the protein was monitored by SDS-PAGE at various times during the incubation. Cleaved protein was then loaded onto a Ni²⁺-NTA agarose column that had been pre-equilibrated with buffer A. The flow through was collected and dialyzed against buffer B containing 1 M NaCl. This sample was then applied to a Sephadex 75 (Amersham Biosciences) gel filtration column. Fractions containing the purified MtRuvC were pooled and dialyzed against storage buffer (20 mM Tris-HCl, pH 8, 1 mM DTT, 50 mM NaCl, 50% glycerol). Purity of MtRuvC was assessed by SDS-PAGE, followed by Coomassie blue staining. The concentration of MtRuvC was determined by the dye binding method using BSA as a standard (Bradford, 1976) and aliquots stored at -80 °C.

Construction of a recombinant plasmid carrying the M. tuberculosis ruvX gene

The *M. tuberculosis ruvX* nucleotide sequence was obtained from the TubercuList database (<http://www.Pasteur.fr/Bio/TubercuList>). The coding sequence, corresponding to *M. tuberculosis* H37Rv *ruvX* gene (Rv2554c) was amplified by PCR from genomic DNA using 5'-AAGGCTAGCGTGGTCCCAACACAGCAC-3' and 5'-GTCAAGCTTTCTGGCATCGGAGCCTTA-3') carrying NheI and HindIII sites (underlined), respectively. The PCR product was gel-purified, digested with NheI and HindIII and inserted into the pET21a(+) expression vector. The resultant plasmid was designated pMtRX.

Construction of M. tuberculosis ruvX substitution mutations

Oligonucleotides used for site-directed mutagenesis are listed in Table S5. The *ruvX* gene of pMtRX was mutated using the QuikChange method with Pfu Turbo DNA polymerase and DpnI. The aspartic acid was replaced by asparagine at position 28 in the RuvX protein sequence; similarly, a cysteine was substituted with alanine at position 38. *E. coli* DH5α

served as the host for plasmid amplification. The mutants were verified by restriction analysis and DNA sequencing.

Overexpression and purification of M. tuberculosis RuvX and mutant derivatives

MtRuvX protein was expressed in the *E. coli* strain Rosetta (DE3)pLysS harbouring pMtRX. Bacteria were grown in LB broth supplemented with antibiotics (100 µg ml⁻¹ ampicillin and 34 µg ml⁻¹ chloramphenicol) at 37 °C until an A₆₀₀ of 0.5. MtRuvX was induced by addition of 0.5 mM IPTG and cultures were further incubated while being shaken gently at 37 °C for 8 h. Cells were collected by centrifugation, washed in STE buffer, resuspended in buffer A and stored at -80 °C. Cells were thawed, sonicated, and the lysate centrifuged as described for MtRuvC. The whole cell lysate was applied onto a SP-Sepharose column pre-equilibrated with buffer A and bound proteins eluted with a 200-600 mM linear gradient of NaCl in buffer A. Fractions containing MtRuvX were pooled and dialyzed against buffer B containing 50 mM NaCl. The sample was then loaded onto a heparin-agarose column pre-equilibrated with buffer B containing 50 mM NaCl. Bound proteins were eluted with a 200-600 mM linear gradient of NaCl in buffer B. The fractions containing MtRuvX were pooled and precipitated by addition of solid ammonium sulfate to 60% saturation. Precipitated proteins were collected by centrifugation at 10000 x g for 25 min at 4 °C. The pellet was resuspended in buffer C (20 mM Tris-HCl, pH 8, 10% glycerol] containing 1 M NaCl and 5 mM 2-mercaptoethanol, and dialyzed against the same buffer. This sample was subjected to gel filtration through a Superdex-75 column. Fractions containing MtRuvX were pooled and dialyzed against storage buffer (20 mM Tris-HCl, pH 8, 50 mM NaCl, 50% glycerol). The purity of MtRuvX was assessed by SDS-PAGE, followed by Coomassie blue staining and aliquots of MtRuvX stored at -80 °C. *M. tuberculosis* RuvX variants, MtRuvX^{D28N} and MtRuvX^{C38A}, were expressed and purified as described for the wild-type MtRuvX. The concentration of wild-type and mutant MtRuvX proteins was determined by the dye binding method using BSA as a standard (Bradford, 1976). Matrix-assisted laser desorption/ionization-time-of-flight (MALDI-TOF) analysis of MtRuvX was carried out using a Bruker Biflex time-of-flight mass spectrometer (Bruker Franzen, Bremen, Germany) according to the manufacturer's recommendations.

Cloning, overexpression and purification of E. coli YqgF

The nucleotide sequence of *E. coli* K-12 *yqgF* was amplified by PCR using Pfx polymerase from genomic DNA using 5'-CAGGACACGCCATATGAGTGGAACC-3' and 5'-CGCCAAGCTTTTAAATCGCCTTAATATC-3' containing NdeI and BamHI restriction sites (underlined). The digested PCR product was inserted into pT7-7 to generate pEcYF. EcYqgF was overexpressed from 2 l of BL21-CodonPlus cells harbouring pEcYF in LB broth supplemented with antibiotics (100 $\mu\text{g ml}^{-1}$ ampicillin and 34 $\mu\text{g ml}^{-1}$ chloramphenicol) at 37 °C. EcYqgF expression was induced in cells at an $A_{650\text{nm}}$ of 0.5 by addition of 1 mM IPTG followed by shaking at 37 °C for a further 3 h. Harvested cells, resuspended in 100 mM Tris-HCl, pH 8, 2 mM EDTA, 5% glycerol, were lysed by sonication, and the lysate was centrifuged at 15000 x g for 20 min at 4 °C. The supernatant was mixed with 50 ml DEAE cellulose and the column developed in buffer A with bound proteins eluted in a linear gradient of 0-1 M mM KCl in buffer A. Pooled fractions containing EcYqgF were subsequently applied to 10 ml heparin-agarose, 4 ml ssDNA cellulose and 1.5 ml phosphocellulose columns with similar elution conditions followed by dialysis into low salt conditions between each chromatography step. A total of 11 mg of purified EcYqgF was recovered and stored in aliquots at -80 °C in storage buffer.

Gel Filtration Chromatography

Analytical size exclusion chromatography was performed using a Superdex 200 10/300GL column (GE Healthcare) with a flow rate of 0.3 ml/min at 18 °C. The column was equilibrated with a buffer containing 20 mM Tris-HCl, pH 8, 200 mM NaCl and 10% glycerol. A set of protein standards of known molecular mass such as RNase A (13.7 kDa), carbonic anhydrase (29 kDa), ovalbumin (43 kDa), conalbumin (137 kDa), apoferritin (480 kDa), and blue dextran (2000 kDa) was used to construct the standard curve. 100 μl of purified protein (1.2 mg/ml) was dialysed in the column equilibration buffer and passed through the column. The fractions were monitored by UV absorbance at 220 nm. The elution volume (V_e) corresponding to the protein peak was determined and the molecular weight was calculated by interpolation on the standard curve.

DNA binding assays

Reaction mixtures (20 μl) contained 20 mM Tris-HCl, pH 8, 100 $\mu\text{g/ml}$ BSA, 0.3-0.5 nM of the indicated 5'- $\gamma^{32}\text{P}$ -labeled DNA and increasing concentrations of MtRuvC, MtRuvX or

EcYqgF. Binding mixtures were incubated at 37 °C for 30 min (MtRuvC and MtRuvX) or on ice for 15 min (EcYqgF). For MtRuvC, the reactions were cross-linked by adding glutaraldehyde to a final concentration of 0.2% and incubating them at 37 °C for 10 min; the reaction was terminated by addition of 2 µl loading dye (0.1% (w/v) of bromophenol blue and xylene cyanol in 20% glycerol). Samples were subjected to electrophoresis through a 4% polyacrylamide gel in 0.25xTBE buffer (6.7 mM Tris-HCl, pH 8, 3.3 mM sodium acetate, 2 mM EDTA) at 75 V for 4 h at 4 °C. Gel was dried, exposed to phosphorimaging screens and bands visualized using a Fuji FLA-9000 phosphorimager or by autoradiography. Data were quantified using the UVitech gel documentation station with UVI-BandMap software (ver. 97.04) and plotted using Graphpad Prism version 5. Statistical data analysis was conducted using a nonlinear regression equation.

Endonuclease activity assays

Typical reaction mixtures (20 µl) contained 20 mM Tris-HCl (pH 8.5), 100 µg ml⁻¹ BSA, 10 mM MgCl₂, and 0.3-0.5 nM 5'- γ ³²P-labeled DNA and MtRuvC, MtRuvX or EcYqgF at the indicated concentrations. Reaction mixtures were incubated at 37 °C for 1 h and terminated by addition of 5 µl of stop solution (2.5% (w/v) SDS, 200 mM EDTA, 10 mg/ml proteinase K), followed by incubation for a further 20 min at 37 °C. Samples were subjected to electrophoresis through an 8% polyacrylamide gel in TBE buffer (90 mM Tris-borate, pH 8, 2 mM EDTA) at 100 V for 5 h at 4 °C. Gels were dried and visualized by autoradiography or phosphorimaging. Band intensities were quantified as described above.

Mapping of MtRuvX cleavage sites

Four HJs, each individually 5'-³²P-labeled on a single strand were incubated with MtRuvX in a buffer containing 20 mM Tris-HCl, pH 8.5, 100 µg ml⁻¹ BSA and 10 mM MgCl₂ at 37 °C for 1 h. Reactions were terminated by addition of 5 µl of stop solution and incubation at 37 °C for 20 min. Samples were extracted with phenol/chloroform, and the DNA precipitated with ethanol. The pellet obtained after centrifugation was resuspended in 5 µl of sequencing loading buffer (0.3% (w/v) bromophenol blue, 0.3% (w/v) xylene cyanol, 10 mM EDTA, pH 7.5, 97.5% (v/v) formamide) and denatured by boiling for 5 min. Samples were analyzed by electrophoresis on a 12% polyacrylamide-8 M urea gel at 1200 V for 2 h (Sambrook *et al.*, 1989). A+G sequencing ladders of each labelled oligonucleotide, generated using the Maxam-

Gilbert method, were loaded alongside to provide markers. Electrophoresis was carried out in 89 mM Tris-borate buffer, pH 8.3, 1 mM EDTA at 1800 V and 40W for 3 h. Gels were dried and analyzed by phosphorimaging. Cleavage sites were mapped with reference to the sequencing ladder. A 1.5 base allowance was made to compensate for the nucleoside eliminated in the sequencing reaction.

Chemical crosslinking of MtRuvX

Purified MtRuvX solution (6 μ M) was dialyzed against a buffer containing 20 mM Tris-HCl, pH 8 and 10% glycerol, and was treated with the indicated amounts of freshly diluted glutaraldehyde. After incubation at 37 °C for 30 min, 5x SDS sample loading buffer (10 mM Tris-HCl, pH 6.8, 40% glycerol, 12.5% SDS, 25 mM DTT, 0.1% bromophenol blue) was added and incubation extended for 5 min at 95 °C. Samples were analyzed by 12.5% SDS-PAGE. The crosslinked and non-cross linked bands were visualized by staining with silver nitrate.

AFM imaging

MtRuvX was diluted to a concentration of 100 nM in 20 mM Tris-HCl, pH 8, 2 mM MgCl₂. Aliquots (5 μ l) of the reaction mixture were deposited on the surface of freshly cleaved mica and were allowed to bind for 5 min. The mica surface was rapidly rinsed with nanopure deionized water and air dried. AFM Images were acquired in tapping mode using an SNL (silicon tip on nitride lever) probe (Agilent Technologies, spring constant 21-98N/M). Molecular masses were derived from the measured volumes as described (Edstrom *et al.*, 1990, Yang *et al.*, 2003).

The volume of molecules was calculated using the equation: $V_m = \pi h/6 (3r^2 + h^2)$, where V_m is the molecular volume, and r and h are the radius and the height of the protein, respectively (Schneider *et al.*, 1995). The theoretical molecular volume of the protein was calculated using the equation: $V_c = M_o/N_o (V_1 + dV_2)$, where M_o is the molecular weight, N_o is Avogadro's number, and V_1 and V_2 are the partial specific volumes of the individual protein (0.74 cm³ g⁻¹ and 1 cm³ g⁻¹ water, respectively) d is the extent of protein hydration (0.4 mol water/mol protein) (Edstrom *et al.*, 1990).

In vitro oxidation of proteins

The assay was conducted essentially as described (Oudot *et al.*, 1999; Indu *et al.*, 2010). Reaction mixtures contained 20 mM Tris-HCl, pH 8, 20 mM NaCl, MtRuvX (0.8 mg ml⁻¹), 5 mM 1,10 phenanthroline and 1.5 mM copper sulfate. After incubation at 20 °C for 24 h, the sample was divided into two fractions; the first fraction was incubated with 20 mM dithiothreitol and the second was retained without further treatment. Both fractions were mixed with SDS-PAGE sample buffer (lacking 2-mercaptoethanol) and heated at 95 °C for 5 min. Samples were analyzed on a 12.5% nonreducing PAGE and protein bands visualized using Coomassie brilliant blue staining. The same procedure was followed for analysis of the MtRuvX^{C38A} mutant.

Acknowledgements

This work was supported by a fellowship to A. N. from the Council of Scientific and Industrial Research, New Delhi, and a grant from the Center of Excellence and Innovation program of the Department of Biotechnology, New Delhi. K. M. is the recipient of a J. C. Bose National Fellowship from the Department of Science and Technology, New Delhi.

Conflict of Interest: none

References

- Aravind, L., K.S. Makarova & E.V. Koonin (2000) Holliday junction resolvases and related nucleases: identification of new families, phyletic distribution and evolutionary trajectories. *Nucleic Acids Res.* **28**, 3417-3432.
- Ariyoshi, M., D. G. Vassylyev, H. Iwasaki, H. Nakamura, H. Shinagawa & K. Morikawa (1994) Atomic structure of the RuvC resolvase: a Holliday junction-specific endonuclease from *E. coli*. *Cell* **78**, 1063-1072.
- Bayburt, T. H. & S. G. Sligar (2002) Single-molecule height measurements on microsomal cytochrome P450 in nanometer-scale phospholipid bilayer disks. *Proc. Natl. Acad. Sci. U.S.A.* **99**, 6725-6730.
- Bennett, R. J., H. J. Dunderdale & S.C. West (1993) Resolution of Holliday junctions by RuvC resolvase: cleavage specificity and DNA distortion. *Cell* **74**, 1021-1031.

- Benson, F. E. & S. C. West (1994) Substrate specificity of the *Escherichia coli* RuvC protein. Resolution of three- and four-stranded recombination intermediates. *J. Biol. Chem.* **269**, 5195-5201.
- Bradford, M. M. (1976) A rapid and sensitive for the quantitation of microgram quantities of protein utilizing the principle of protein-dye binding, *Anal. Biochem.* **72**, 248-254.
- Brooks, P.C., F. Movahedzadeh & E.O. Davis (2001) Identification of some DNA damage inducible genes of *Mycobacterium tuberculosis*: apparent lack of correlation with LexA binding. *J. Bacteriol.* **183**, 4459-4467.
- Careaga, C.L & J. J. Falke (1992) Thermal motions of surface alphahelices in the D868 galactose chemosensory receptor. Detection by disulfide trapping. *J. Mol. Biol.* **226**, 1219-1235.
- Chan, S. N., L. Harris, E. L. Bolt, M. C. Whitby & R. G. Lloyd (1997) Sequence specificity and biochemical characterization of the RusA Holliday junction resolvase of *Escherichia coli*. *J. Biol. Chem.* **272**, 4873-14882.
- Chen, L., K. Shi, Z. Yin & H. Aihara (2013) Structural asymmetry in the *Thermus thermophilus* RuvC dimer suggests a basis for sequential strand cleavages during Holliday junction resolution. *Nucleic Acids Res.* **41**, 648-656.
- Dunderdale, H. J., F. E. Benson, C. A. Parsons, G.J. Sharples, R. G. Lloyd & S. C. West (1991) Formation and resolution of recombination intermediates by *E. coli* RecA and RuvC proteins. *Nature* **354**, 506-510.
- Edstrom, R. D., M. H. Meinke, X. R. Yang, R. Yang, V. Elings & D. F. Evans (1990) Direct visualization of phosphorylase-phosphorylase kinase complexes by scanning tunnelling and atomic force microscopy. *Biophys. J.* **58**, 1437-1448.
- Freiberg, C., B. Wieland, F. Spaltmann, 882 K. Ehlert, H. Brötz & H. Labischinski (2001) Identification of novel essential *Escherichia coli* genes conserved among pathogenic bacteria. *J. Mol. Microbiol. Biotechnol.* **3**, 483-489.
- Fu, L. M. & C. S. Fu-Liu (2007). The gene expression data of *Mycobacterium tuberculosis* based on Affymetrix gene chips provide insight into regulatory and hypothetical genes. *BMC Microbiol.* **7**, 37.
- Galperin, M. Y., D. J. Rigden & X. M. Fernández-Suárez (2015) The 2015 Nucleic Acids Research Database Issue and molecular biology database collection. *Nucl Acids Res. Database Issue* **42**, D222-D230.
- Giraud-Panis, M.-J. E., D. R. Duckett & D. M. J. Lilley (1995) The modular character of a DNA junction resolving enzyme: a zinc binding motif in T4 endonuclease VII. *J. Mol. Biol.* **252**, 596-610.

Gorecka, K.M., W. Komorowska & M. Nowotny (2013) Crystal structure of RuvC resolvase in complex with Holliday junction substrate. *Nucleic Acids Research* **41**, 9945- 9955.

Habeeb, A.J. & R. Hiramoto (1968) Reaction of proteins with glutaraldehyde. *Arch. Biochem. Biophys.* **126**, 16-26.

Han Y.W., T. Tani, M. Hayashi, T. Hishida, H. Iwasaki, H. Shinagawa & Y. Harada (2006) Direct observation of DNA rotation during branch migration of Holliday junction DNA by *Escherichia coli* RuvA-RuvB protein complex. *Proc. Natl. Acad. Sci. U.S.A.* **103**, 11544-11548.

Hidalgo, A. A., A.N. Trombert, J. C. Castro-Alonso, C. A. Santiviago, B. R. Tesser, P. Youderian & G. C. Mora (2004). Insertions of mini-Tn10 transposon T-POP in *Salmonella enterica* sv. typhi. *Genetics* **167**, 1069-1077.

Indu, S., S. T. Kumar, S. Thakurela, M. Gupta, R. M. Bhaskara, C. Ramakrishnan & R. Varadarajan (2010) Disulfide conformation and design at helix N-termini. *Proteins* **78**, 1228-1242.

Iwamoto, A., A. Osawa, M. Kawai, H. Honda, S. Yoshida, N. Furuya & J. Kato (2012). Mutations in the essential *Escherichia coli* gene, *yqgF*, and their effects on transcription. *J. Mol. Microbiol. Biotechnol.* **22**, 17-23.

Iwasaki, H., M. Takahagi, T. Shiba, A. Nakata & H. Shinagawa (1991) *Escherichia coli* RuvC protein is an endonuclease that resolves the Holliday structure. *EMBO J.* **10**, 4381- 4389.

Komori, K., S. Sakae, R. Fujikane, K. Morikawa, H. Shinagawa & Y. Ishino (2000) Biochemical characterization of the Hjc Holliday junction resolvase of *Pyrococcus furiosus*. *Nucleic Acids Res.* **28**, 4544-4551.

Kowalczykowski, S.C. (2000) Initiation of genetic recombination and recombination dependent replication. *Trends Biochem. Sci.* **25**, 156-165.

Kurata, T., S. Nakanishi, M. Hashimoto, M. Taoka, Y. Yamazaki, T. Isobe & J. Kato (2015) Novel essential gene involved in 16S rRNA processing in *Escherichia coli*. *J. Mol. Biol.* **427**, 955-965.

Lilley, D. M. J. & M. F. White (2000) Resolving the relationships of resolving enzymes. *Proc. Natl. Acad. Sci. U.S.A.* **97**, 9351-9353.

Lilley, D. M. J. & M. F. White (2001) The junction-resolving enzymes. *Nat. Rev. Mol. Cell Biol.* **2**, 433-443.

Liu, X., M. M. Gutacker, J.M. Musser & Y.X. Fu (2006) Evidence for recombination in *Mycobacterium tuberculosis*. *J. Bacteriol.* **188**, 8169-8177.

Liu D, Y.S. Wang & D.F. Wyss (2003) Solution structure of the hypothetical protein YqgF from *Escherichia coli* reveals an RNase H fold. *J. Biomol. NMR* **27**, 389-392.

Lloyd, R.G. & G. J. Sharples (1993) Processing of recombination intermediates by the RecG and RuvAB proteins of *Escherichia coli*. *Nucleic Acids Res.* **21**, 1719-1725.

Long, Q., Q. Du, T. Fu, K. Drlica, X. Zhao & J. Xie (2015) Involvement of Holliday junction resolvase in fluoroquinolone-mediated killing of *Mycobacterium smegmatis*. *Antimicrob. Agents Chemother.* **59**, 1782-1785.

Maxam A.M. & W. Gilbert (1980) Sequencing end-labeled DNA with base-specific chemical cleavages. *Methods Enzymol.* **65**, 499-560.

McFadden, J. (1996) Recombination in mycobacteria. *Mol. Microbiol.* **21**, 205-211.

McGlynn, P. & R. G. Lloyd (2000) Modulation of RNA polymerase by (p)ppGpp reveals a RecG-dependent mechanism for replication fork progression. *Cell* **101**, 35-45.

Michel, B. (2000). Replication fork arrest and DNA recombination. *Trends Biochem. Sci.* **25**, 173-178.

Movahedzadeh, F., M.J. Colston & E.O. David (1997) Determination of DNA sequences required for regulated *Mycobacterium tuberculosis* RecA expression in response to DNA damaging agents suggests that two modes of regulation exist. *J. Bacteriol.* **179**, 3509- 3518.

Muniyappa, K., M.B. Vaze, N. Ganesh, M. Sreedhar Reddy, N. Guhan & R. Venkatesh (2000). Comparative genomics of *Mycobacterium tuberculosis* and *Escherichia coli* for recombination (*rec*) genes. *Microbiology* **146**, 2093-2095.

Mizrahi, V. & S.J. Andersen (1998) DNA repair in *Mycobacterium tuberculosis*. What have we learnt from the genome sequence? *Mol. Microbiol.* **29**, 1331-1339.

Nowotny M. (2009) Retroviral integrase superfamily: the structural perspective. *EMBO Rep.* **10**, 144-151.

Oram, M., A. Keeley & I. Tsaneva (1998) Holliday junction resolvase in *Schizosaccharomyces pombe* has identical endonuclease activity to the CCE1 homologue YDC2. *Nucleic Acids Res.* **26**, 594-601.

Oudot, C.M. Jaquinod, J.C. Cortay, A.J. Cozzone & J.M. Jault (1999). The isocitrate dehydrogenase kinase/phosphatase from *Escherichia coli* is highly sensitive to *in-vitro* oxidative conditions role of cysteine67 and cysteine108 in the formation of a disulfide bonded homodimer. *Eur. J. Biochem.* **262**, 224-229.

Pérez-Martín, J. & V. de Lorenzo (1996) ATP binding to the sigma 54-dependent activator XylR triggers a protein multimerization cycle catalyzed by UAS DNA. *Cell* **86**, 331-339.

Ponting, C.P. (2002). Novel domains and orthologues of eukaryotic transcription elongation factors. *Nucleic Acids Res.* **30**, 3643-3652.

Rand, L., J. Hinds, B. Springer, P. Sander, R.S. Buxton & E. O. Davis (2003) The majority of inducible DNA repair genes in *Mycobacterium tuberculosis* are induced independently of RecA. *Mol. Microbiol.* **50**, 1031-1042.

Rosas-Magallanes, V., P. Deschavanne, L. Quintana-Murci, R. Brosch, B. Gicquel & Neyrolles, O. (2006) Horizontal transfer of a virulence operon to the ancestor of *Mycobacterium tuberculosis*. *Mol. Biol. Evol.* **23**, 1129-1135.

Saito, A., H. Iwasaki, M. Ariyoshi, K. Morikawa & H. Shinagawa (1995) Identification of four acidic amino acids that constitute the catalytic center of the RuvC Holliday junction resolvase. *Proc. Natl. Acad. Sci. U. S. A.* **92**, 7470-7474.

Sambrook, J., E.F. Fritsch & T. Maniatis (1989) *Molecular Cloning: A Laboratory Manual*, 2nd Edition, Cold Spring Harbor Laboratory Press, Cold Spring Harbor, New York.

Sasseti, C. M., D. H. Boyd & E. J. Rubin (2003) Genes required for mycobacterial growth defined by high density mutagenesis. *Mol. Microbiol.* **48**, 77-84.

Schneider, S., Folprecht, G., Krohne, G. & H. Oberleithner (1995) Immunolocalization of lamins and nuclear pore complex proteins by atomic force microscopy. *Pflügers Arch* **430**, 795–801.

Seigneur, M., V. Bidnenko, S. D. Ehrlich & B. Michel (1998) RuvAB acts at arrested replication forks. *Cell* **95**, 419-430.

Shah, R., R. J. Bennett & S. C. West (1994a) Genetic recombination in *E. coli*: RuvC protein cleaves Holliday junction at resolution hotspots *in vitro*. *Cell* **79**, 853-864.

Shah, R., R. J. Bennett & S.C. West (1994b) Activation of RuvC Holliday junction resolvase *in vitro*. *Nucleic Acids Res.* **22**, 2490-2497.

Sharples, G. J. (2001) The X philes: structure-specific endonucleases that resolve Holliday junctions. *Mol. Microbiol.* **39**, 823-834.

Sharples, G. J., S. N. Chan, A. A. Mahdi, M. C. Whitby & R. G. Lloyd (1994) Processing of intermediates in recombination and DNA repair: identification of a new endonuclease that specifically cleaves Holliday junctions. *EMBO J.* **13**, 6133-6142.

Sharples, G. J., L. M. Corbett & I. R. Graham (1998) Lambda Rap protein is a structure specific endonuclease involved in phage recombination. *Proc. Natl. Acad. Sci. U. S. A.* **95**, 13507-13512.

Sharples, G. J., E. L. Bolt & R. G. Lloyd (2002) RusA proteins from the extreme thermophile *Aquifex aeolicus* and lactococcal phage ρ 1t resolve Holliday junctions. *Mol. Microbiol.* **44**, 549-559.

Shinagawa, H. & H. Iwasaki (1996). Processing the Holliday junction in homologous recombination. *Trends Biochem. Sci.* **21**, 107-111.

Thakur, R.S., S. Basavaraju, K. Somyajit, A. Jain, K. Muniyappa & G. Nagaraju (2013) Evidence for the role *Mycobacterium tuberculosis* RecG helicase in DNA repair and recombination. *FEBS J.* **280**, 1841–1860.

Vultos, T.D., O. Mestre, T. Tonjum & B. Gicquel (2009) DNA repair in *Mycobacterium tuberculosis* revisited. *FEMS Microbiol. Rev.* **33**, 471–487.

White, M.F., E. Marie-Josèphe, J. Giraud-Panis, J., 1008 R.G. Pöhler & Lilley, D.M.J. (1997). Recognition and manipulation of branched DNA structure by junction-resolving enzymes. *J. Mol. Biol.* **269**, 647-664.

West, S.C. (1996). The RuvABC proteins and Holliday junction processing in *Escherichia coli*. *J. Bacteriol.* **178**, 1237-1241.

West, S.C. (1997). Processing of recombination intermediates by the RuvABC proteins *Annu. Rev. Genet.* **31**, 213-244.

Whitby, M.C., L. Ryder & R.G. Lloyd (1993) Reverse branch migration of Holliday junction by RecG protein: a new mechanism for resolution of intermediates in recombination and DNA repair. *Cell* **75**, 341-350.

White, M. F. & D. M. J. Lilley (1996) The structure-selectivity and sequence-preference of the junction-resolving enzyme CCE1 of *Saccharomyces cerevisiae*. *J. Mol. Biol.* **257**, 330-341.

White, M. F., M. J. Giraud-Panis, J. R. Pöhler & D. M. J. Lilley (1997) Recognition and manipulation of branched DNA structure by junction-resolving enzymes. *J. Mol. Biol.* **269**, 647-664.

Wyatt, H. D. & S. C. West (2014). Holliday junction resolvases. *Cold Spring Harb. Perspect. Biol.* **6**, a023192.

Yang, Y., H. Wang & Erie, D. A. (2003) Quantitative characterization of biomolecular assemblies and interactions using atomic force microscopy. *Methods* **29**, 175–187.

Zhang, X.S. & M. J. Blaser (2012). DprB facilitates inter- and intragenomic recombination in *Helicobacter pylori*. *J. Bacteriol.* **194**, 3891-3903.

Figure Legends

Figure 1. Expression levels of *M. tuberculosis* *ruvC*, *ruvX* and *recA* in response to DNA damaging agents. The data show transcriptional changes after exposure to MMS (A) or 180 J/m² UV light (B). Quantitative real-time PCR was used to determine expression levels in untreated control cells and in response to MMS and UV radiation treatment. Each data set represents the mean and standard deviation from three independently isolated RNA samples. The levels of expression were determined and normalized to 16S ribosomal RNA expression and induction ratios (fold increase) calculated relative to the untreated control.

Figure 2. Holliday junction binding and resolution activities of MtRuvC and MtRuvX. The gels show binding and cleavage activities of MtRuvC (A and C) and MtRuvX (B and D), respectively, on a 12 bp mobile HJ. Reaction mixtures in (A) contained 0.5 nM ³²P-labeled HJ12 in the absence (lane 1) or presence (lanes 2-8) of 200, 400, 600, 800, 900, 1000 and 2000 nM MtRuvC, respectively. Reaction mixtures in (B) contained 0.5 nM ³²P-labeled HJ12 in the absence (lane 1) or presence (lanes 2-8) of 25, 50, 100, 150, 200, 300, 400 nM MtRuvX, respectively. An asterisk denotes the strand in HJ12 labeled with ³²P. In (C) and (D), lane 1 (m) contained ³²P-labeled linear duplex DNA; lane 2, a no protein control with HJ12; and lanes 3-9, complete reactions containing MtRuvC or MtRuvX at the same concentrations as indicated above.

Figure 3. Characterisation of MtRuvX endonuclease activity. (A) Effect of divalent cations. Assays were conducted in binding buffer containing 0.5 nM ³²P-labeled HJ12 DNA and 500 nM MtRuvX in the absence (lane 1) or presence of 2.5, 5 or 10 mM of Mg²⁺ (lanes 2-4), Mn²⁺ (lanes 5-7) or Zn²⁺ (lanes 8-10). (B) Effect of pH. Assays were conducted in the binding buffer containing 0.5 nM ³²P-labeled HJ12, 500 nM MtRuvX and 10 mM MgCl₂ at the indicated pH (lanes 2-9). (C) Effect of incubation temperature. Assays were conducted in binding buffer containing 0.5 nM ³²P-labeled HJ12, 500 nM MtRuvX and 10 mM MgCl₂ at the indicated incubation temperature (lanes 2-6). (D) Effect of NaCl. Assays were conducted in binding buffer containing 0.5 nM ³²P-labeled HJ12, 500 nM MtRuvX and 10 mM MgCl₂ in the absence (lane 2) or presence of 25, 50, 75, 100, 200, 300, 400, 500 and 600 mM NaCl (lanes 2-11).

Figure 4. MtRuvX displays selectivity for HJ over other DNA recombination intermediates. (A-F) Reaction mixtures contained 0.5 nM ^{32}P -labeled DNA and were incubated in the absence (lane 1) or presence of 25, 50, 100, 125, 150, 175, 250, 500, 750, 1000 nM MtRuvX (lanes 2-11), respectively. Samples were incubated at 37 °C for 30 min and analyzed following electrophoresis on native polyacrylamide gels. An asterisk denotes the ^{32}P -labeled strand in each of the substrates tested. These were a HJ containing a 12 bp homologous core (A), replication fork (B), 5' flap (C), 3' flap (D), splayed duplex (E) and linear duplex (F). A binding isotherm of MtRuvX binding to each of the DNA substrates is shown in (G); error bars represent the mean and standard deviation from three independent experiments.

Figure 5. Sensitivity of MtRuvX-DNA complexes to salt. (A) HJ12 containing a 12 bp homologous core, (B) replication fork and (C) linear duplex DNA. Binding mixtures contained 0.5 nM ^{32}P -labeled DNA and 1000 nM of MtRuvX. Lane 1, DNA without protein; lane 2, DNA with MtRuvX in the absence of salt; lanes 3-11, DNA with MtRuvX in the presence of 25, 50, 75, 100, 125, 150, 175, 200 and 250 mM NaCl. Samples were analyzed on native polyacrylamide gels and visualized by phosphorimaging. (D) Graphic representation of the extent of dissociation of MtRuvX-DNA complexes with increasing NaCl concentration. The data points represent the mean and standard deviation of three independent experiments.

Figure 6. MtRuvX activity on mobile and immobile Holliday junctions. (A) Representative band shift assay of MtRuvX binding to HJ12, a HJ containing a 12 bp mobile core (B) Representative band shift assay of MtRuvX binding to an immobile HJ, HJ0. Reaction mixtures in (A) and (B) contained 0.5 nM ^{32}P -labeled HJ incubated in the absence (lane 1) or presence (lanes 2-11) of 25, 50, 100, 125, 150, 175, 250, 500, 750 and 1000 nM MtRuvX, respectively. Samples were incubated at 37 °C for 30 min and analyzed by electrophoresis on native polyacrylamide gels. An asterisk denotes the strand labeled with ^{32}P in each substrate; the HJ structure with a boxed area indicates the immobile core in HJ0. (C-E) Reaction mixtures contained 0.5 nM of the indicated ^{32}P -labeled DNA substrate in the absence (lane 1) or presence (lanes 2-12) of 25, 50, 75, 100, 125, 150, 175, 200, 250, 300 and 500 nM MtRuvX. After incubation at 37 °C for 60 min, samples were analyzed on native polyacrylamide gels. Reactions were performed with a mobile HJ (C), an immobile HJ (D) or with linear duplex DNA (E). (F) Graphical representation of the extent of DNA substrate

cleavage on each of the three substrates. Each point on the graph represents the mean and standard deviation of three independent experiments.

Figure 7. Mapping the cleavage sites of MtRuvX on a mobile Holliday junction. (A-D) Reaction mixtures were incubated with four HJ12 substrates (0.5 nM), each ^{32}P -labeled in a different strand (indicated by an asterisk and numbered) in the absence (lane 2) or presence (lanes 3-5) of increasing concentrations of MtRuvX. Lane 1, Maxam-Gilbert G+A sequencing ladder; lane 2, untreated HJ substrate; lanes 3-5, HJ incubated with 100, 150 and 250 nM MtRuvX. A schematic of the central portion of the HJ is depicted at the center with the 12 bp homologous core indicated in red. Cleavage sites are indicated by arrow heads with minor sites in strands 1 and 3 in green and major sites in strands 2 and 4 in blue.

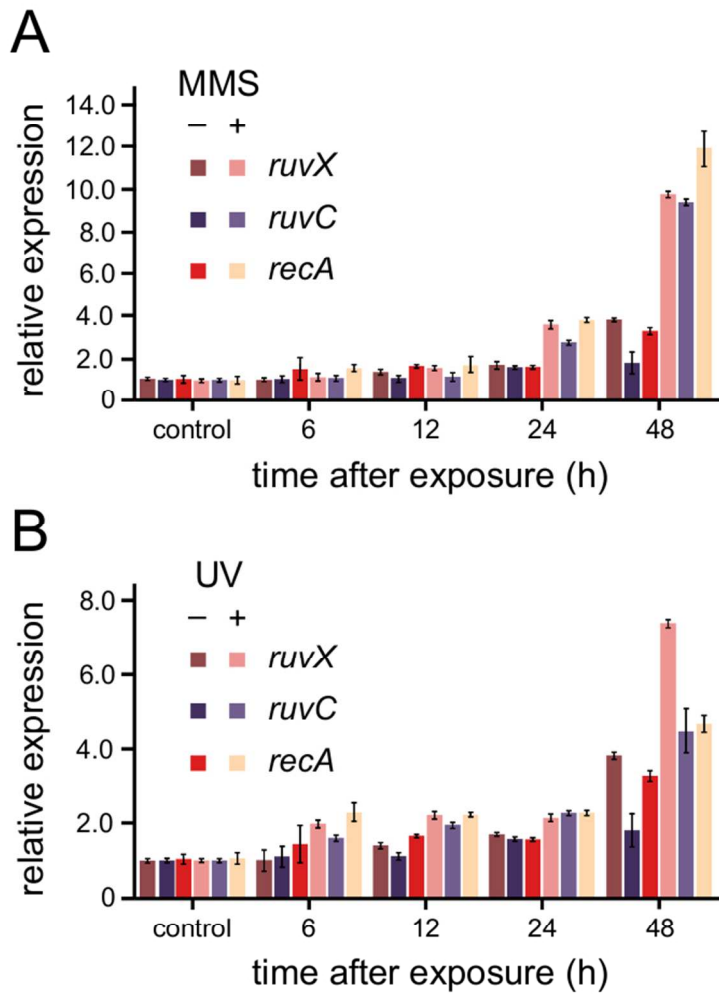
Figure 8. MtRuvX^{D28N} purification and analysis of HJ binding and resolution activity. (A) 12.5% SDS-PAGE summarising the overexpression and purification of *M. tuberculosis* RuvX^{D28N}. Lane 1, molecular mass markers; lane 2, supernatant from uninduced (–) cells; lane 3, supernatant from induced (+) cells; lane 4, pooled fractions from SP-Sepharose; lane 5, pooled fractions from a heparin-agarose column and lane 6, pooled fractions from Sephadex 75 gel filtration chromatography. (B and C) Comparison of HJ12 binding activities of MtRuvX and MtRuvX^{D28N}. Binding mixtures contained 0.5 nM ^{32}P -labeled HJ12 incubated in the absence (lane 1) or presence (lanes lanes 2-11) of 25, 50, 100, 125, 150, 175, 250, 500, 750 and 1000 nM MtRuvX (B) or MtRuvX^{D28N} (C). After incubation at 37 °C for 30 min, samples were analyzed by electrophoresis on native polyacrylamide gels. (D) Graphical representation of MtRuvX and HJ-MtRuvX^{D28N} binding to HJ12. (E and F) HJ resolution activity of MtRuvX and MtRuvX^{D28N}. Reaction mixtures contained 0.5 nM ^{32}P -labeled HJ12 with no protein (lane 1) or with 25, 50, 75, 100, 125, 150, 175, 200, 250, 300 and 500 nM MtRuvX (E, lanes 2-12) or MtRuvX^{D28N} (F, lanes 2-12). After incubation at 37 °C for 60 min, samples were analyzed on native polyacrylamide gels. (G) Graphical representation of HJ cleavage by MtRuvX and MtRuvX^{D28N} quantified from the gels shown in (E) and (F).

Figure 9. MtRuvX exists as a homodimer *in vitro* and *in vivo*. (A) Chemical crosslinking of MtRuvX. Lane 1, molecular mass markers; 2, MtRuvX incubated in the absence of glutaraldehyde; lanes 3-8, MtRuvX incubated with 0.025%, 0.029%, 0.033%, 0.037%, 0.045% and 0.050%, respectively. (B) Upper panel, AFM image of MtRuvX; lower panel, three-dimensional image of MtRuvX on the mica surface. Yellow and white arrows indicate

dimeric and monomeric forms of MtRuvX, respectively. (C) Immunoblot analysis of MtRuvX from *M. tuberculosis* whole cell extracts. Exponentially growing *M. tuberculosis* H37Ra cells were lysed and increasing concentrations of protein loaded on a native gel (lanes 1-4) and probed by Western blotting using anti-MtRuvX polyclonal antibodies. Purified MtRuvX was used as a positive control (lane 5). (D) Gel filtration analysis of MtRuvX. The Superdex 200 10/300GL column was calibrated using molecular weight markers. MtRuvX homodimer eluted after 15.4 ml, consistent with a species of a ~55 kDa, reflecting an elongated monomer. MtRuvX monomer eluted after 16.8 ml, consistent with a ~25 kDa species corresponding to a monomer.

Figure 10. MtRuvX is cross-linked by an intermolecular disulfide bond. (A) 12.5% SDS PAGE of MtRuvX in oxidized and reduced conditions. Lane 1, molecular mass markers; lane 2, control MtRuvX without treatment; lane 3, MtRuvX incubated with 1,10-phenanthroline (PHEN); lane 4, MtRuvX incubated with cupric orthophenanthroline; lane 5, MtRuvX incubated with DTT. The gel was stained with Coomassie blue (B) 12.5% SDS-PAGE of MtRuvX^{C38A} in oxidized and reduced conditions. Lane 1, molecular mass markers; lane 2, control MtRuvX^{C38A} without treatment; lane 3, MtRuvX^{C38A} incubated with DTT; lane 4, MtRuvX^{C38A} incubated with cupric orthophenanthroline; lane 5. The gel was stained with Coomassie blue. (C) HJ binding activity of MtRuvX^{C38A}. Binding mixtures contained 0.5 nM ³²P-labeled HJ12 in the absence (lane 1) or presence (lanes 2-10) of 25, 50, 100, 125, 175, 250, 500, 750 and 1000 nM MtRuvX^{C38A}. (D) HJ resolution activity of MtRuvX^{C38A}. Reaction mixtures contained 0.5 nM ³²P-labeled HJ12 substrate and 10 mM MgCl₂ in the absence (lane 1) or presence (lanes 2-11) of 25, 50, 75, 100, 125, 150, 175, 200, 250, 300 and 500 nM MtRuvX^{C38A}. (E) DTT inhibits HJ resolution activity of MtRuvX. Assay was performed as described above in the absence (lane 2) or presence of 2.5, 5, 10 and 15 mM DTT in lanes 3-6, respectively.

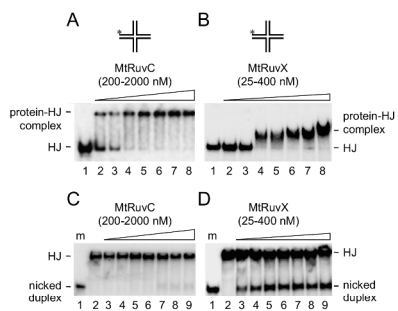
Figure 1



61x94mm (300 x 300 DPI)

AC

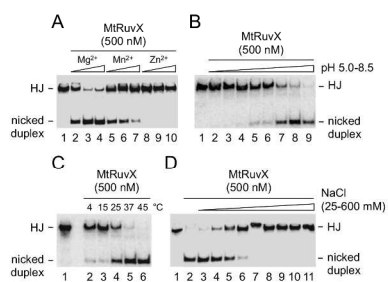
Figure 2



209x297mm (300 x 300 DPI)

AC

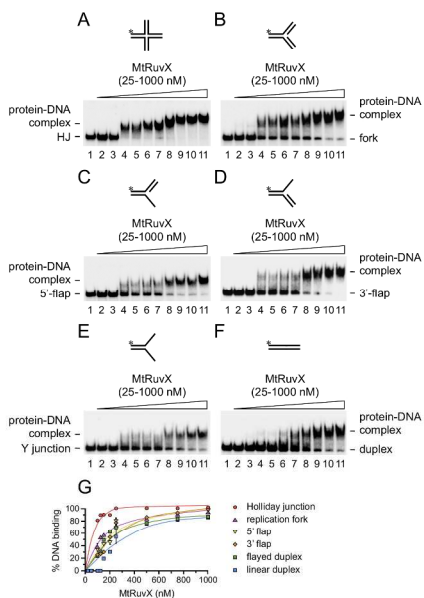
Figure 3



209x297mm (300 x 300 DPI)

AC

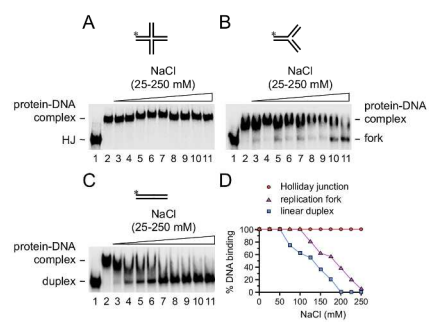
Figure 4



209x297mm (300 x 300 DPI)

AC

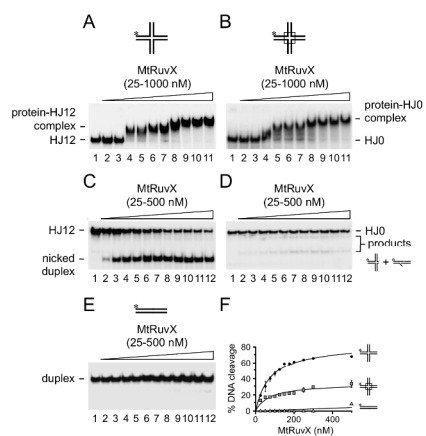
Figure 5



209x297mm (300 x 300 DPI)

AC

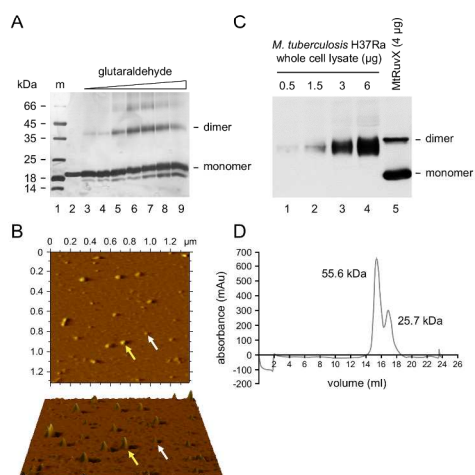
Figure 6



209x297mm (300 x 300 DPI)

AC

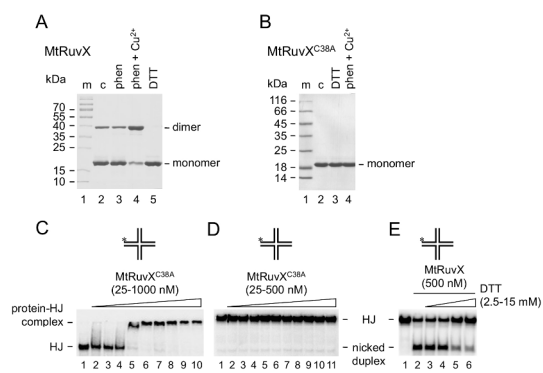
Figure 9



209x297mm (300 x 300 DPI)

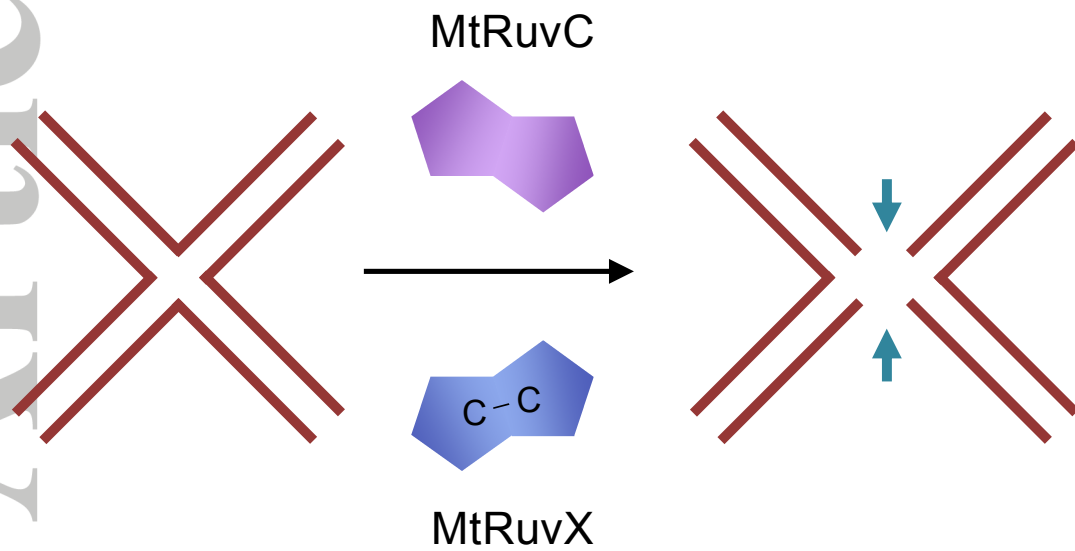
AC

Figure 10



209x297mm (300 x 300 DPI)

AC



***Mycobacterium tuberculosis* uses an unprecedented mechanism for the assembly of the Holliday junction resolvase**

Abbreviated summary

Mycobacterium tuberculosis genome possesses homologues of the *ruvC* and *ruvX* (*yqgF*) genes that encode putative Holliday junction (HJ) resolvases. However, their enzymatic properties have not been experimentally defined. This work reveals that although both MtRuvC and MtRuvX cleaved HJ, the latter displayed robust HJ resolution activity. Strikingly, we found that disulfide-bond mediated dimerization is essential for MtRuvX activity. This is the first example of a Holliday junction resolvase requiring inter-molecular disulfide-bond formation for biological activity.